



Harris hawks optimization: Algorithm and applications

Ali Asghar Heidari^{a,b}, Seyedali Mirjalili^c, Hossam Faris^d, Ibrahim Aljarah^d, Majdi Mafarja^e, Huiling Chen^{f,*}



^a School of Surveying and Geospatial Engineering, University of Tehran, Tehran, Iran

^b Department of Computer Science, School of Computing, National University of Singapore, Singapore

^c School of Information and Communication Technology, Griffith University, Nathan, Brisbane, QLD 4111, Australia

^d King Abdullah II School for Information Technology, The University of Jordan, Amman, Jordan

^e Department of Computer Science, Birzeit University, POBox 14, West Bank, Palestine

^f Department of Computer Science, Wenzhou University, Wenzhou 325035, China

HIGHLIGHTS

- A mathematical model is proposed to simulate the hunting behavior of Harris' Hawks.
- An optimization algorithm is proposed using the mathematical model.
- The proposed HHO algorithm is tested on several benchmarks.
- The performance of HHO is also examined on several engineering design problems.
- The results show the merits of the HHO algorithm as compared to the existing algorithms.

ARTICLE INFO

Article history:

Received 2 June 2018

Received in revised form 29 December 2018

Accepted 18 February 2019

Available online 28 February 2019

Keywords:

Nature-inspired computing

Harris hawks optimization algorithm

Swarm intelligence

Optimization

Metaheuristic

ABSTRACT

In this paper, a novel population-based, nature-inspired optimization paradigm is proposed, which is called Harris Hawks Optimizer (HHO). The main inspiration of HHO is the cooperative behavior and chasing style of Harris' hawks in nature called surprise pounce. In this intelligent strategy, several hawks cooperatively pounce a prey from different directions in an attempt to surprise it. Harris hawks can reveal a variety of chasing patterns based on the dynamic nature of scenarios and escaping patterns of the prey. This work mathematically mimics such dynamic patterns and behaviors to develop an optimization algorithm. The effectiveness of the proposed HHO optimizer is checked, through a comparison with other nature-inspired techniques, on 29 benchmark problems and several real-world engineering problems. The statistical results and comparisons show that the HHO algorithm provides very promising and occasionally competitive results compared to well-established metaheuristic techniques. Source codes of HHO are publicly available at <http://www.alimirjalili.com/HHO.html> and <http://www.evo-ml.com/2019/03/02/hho>.

© 2019 Elsevier B.V. All rights reserved.

1. Introduction

Many real-world problems in machine learning and artificial intelligence have generally a continuous, discrete, constrained or unconstrained nature [1,2]. Due to these characteristics, it is hard to tackle some classes of problems using conventional mathematical programming approaches such as conjugate gradient, sequential quadratic programming, fast steepest, and quasi-Newton methods [3,4]. Several types of research have verified that these methods are not efficient enough or always efficient in dealing

with many larger-scale real-world multimodal, non-continuous, and non-differentiable problems [5]. Accordingly, metaheuristic algorithms have been designed and utilized for tackling many problems as competitive alternative solvers, which is because of their simplicity and easy implementation process. In addition, the core operations of these methods do not rely on gradient information of the objective landscape or its mathematical traits. However, the common shortcoming for the majority of metaheuristic algorithms is that they often show a delicate sensitivity to the tuning of user-defined parameters. Another drawback is that the metaheuristic algorithms may not always converge to the global optimum. [6]

In general, metaheuristic algorithms have two types [7]; single solution based (i.g. Simulated Annealing (SA) [8]) and population-based (i.g. Genetic Algorithm (GA) [9]). As the name indicates, in the former type, only one solution is processed during the optimization phase, while in the latter type, a set of solutions

* Corresponding author.

E-mail addresses: as_heidari@ut.ac.ir, aliasgha@comp.nus.edu.sg, t0917038@u.nus.edu (A.A. Heidari), seyedali.mirjalili@griffithuni.edu.au (S. Mirjalili), hossam.faris@ju.edu.jo (H. Faris), i.aljarah@ju.edu.jo (I. Aljarah), mmafarja@birzeit.edu (M. Mafarja), chenhuiling.jlu@gmail.com, chenhuiling_jsj@wzu.edu.cn (H. Chen).

(i.e. population) are evolved in each iteration of the optimization process. Population-based techniques can often find an optimal or suboptimal solution that may be same with the exact optimum or located in its neighborhood. Population-based metaheuristic (P-metaheuristics) techniques mostly mimic natural phenomena [10–13]. These algorithms start the optimization process by generating a set (population) of individuals, where each individual in the population represents a candidate solution to the optimization problem. The population will be evolved iteratively by replacing the current population with a newly generated population using some often stochastic operators [14,15]. The optimization process is proceeded until satisfying a stopping criteria (i.e. maximum number of iterations) [16,17].

Based on the inspiration, P-metaheuristics can be categorized in four main groups [18,19] (see Fig. 1): Evolutionary Algorithms (EAs), Physics-based, Human-based, and Swarm Intelligence (SI) algorithms. EAs mimic the biological evolutionary behaviors such as recombination, mutation, and selection. The most popular EA is the GA that mimics the Darwinian theory of evolution [20]. Other popular examples of EAs are Differential Evolution (DE) [21], Genetic Programming (GP) [20], and Biogeography-Based Optimizer (BBO) [22]. Physics-based algorithms are inspired by the physical laws. Some examples of these algorithms are Big-Bang Big-Crunch (BBC) [23], Central Force Optimization (CFO) [24], and Gravitational Search Algorithm (GSA) [25]. Salcedo-Sanz [26] has deeply reviewed several physic-based optimizers. The third category of P-metaheuristics includes the set of algorithms that mimic some human behaviors. Some examples of the human-based algorithms are Tabu Search (TS) [27], Socio Evolution and Learning Optimization (SELO) [28], and Teaching Learning Based Optimization (TLBO) [29]. As the last class of P-metaheuristics, SI algorithms mimic the social behaviors (e.g. decentralized, self-organized systems) of organisms living in swarms, flocks, or herds [30,31]. For instance, the birds flocking behaviors is the main inspiration of the Particle Swarm Optimization (PSO) proposed by Eberhart and Kennedy [32]. In PSO, each particle in the swarm represents a candidate solution to the optimization problem. In the optimization process, each particle is updated with regard to the position of the global best particle and its own (local) best position. Ant Colony Optimization (ACO) [33], Cuckoo Search (CS) [34], and Artificial Bee Colony (ABC) are other examples of the SI techniques.

Regardless of the variety of these algorithms, there is a common feature: the searching steps have two phases: exploration (diversification) and exploitation (intensification) [26]. In the exploration phase, the algorithm should utilize and promote its randomized operators as much as possible to deeply explore various regions and sides of the feature space. Hence, the exploratory behaviors of a well-designed optimizer should have an enriched-enough random nature to efficiently allocate more randomly-generated solutions to different areas of the problem topography during early steps of the searching process [35]. The exploitation stage is normally performed after the exploration phase. In this phase, the optimizer tries to focus on the neighborhood of better-quality solutions located inside the feature space. It actually intensifies the searching process in a local region instead of all-inclusive regions of the landscape. A well-organized optimizer should be capable of making a reasonable, fine balance between the exploration and exploitation tendencies. Otherwise, the possibility of being trapped in local optima (LO) and immature convergence drawbacks increases.

We have witnessed a growing interest and awareness in the successful, inexpensive, efficient application of EAs and SI algorithms in recent years. However, referring to No Free Lunch (NFL) theorem [36], all optimization algorithms proposed so-far show an equivalent performance on average if we apply

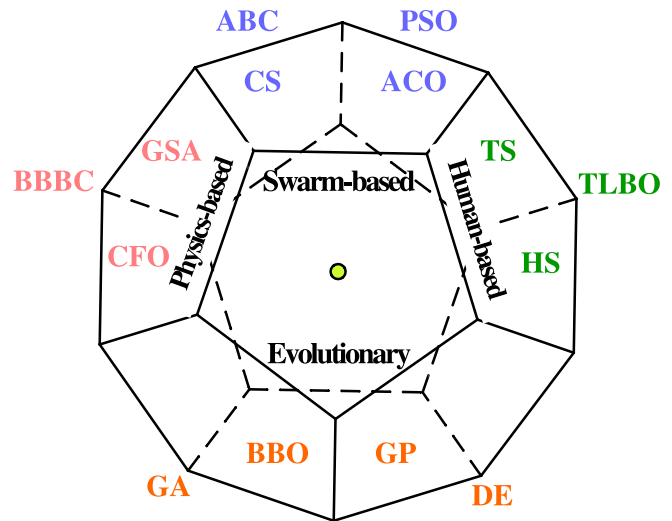


Fig. 1. Classification of meta-heuristic techniques (meta-heuristic diamond).

them to all possible optimization tasks. According to NFL theorem, we cannot theoretically consider an algorithm as a general-purpose universally-best optimizer. Hence, NFL theorem encourages searching for developing more efficient optimizers. As a result of NFL theorem, besides the widespread studies on the efficacy, performance aspects and results of traditional EAs and SI algorithms, new optimizers with specific global and local searching strategies are emerging in recent years to provide more variety of choices for researchers and experts in different fields.

In this paper, a new nature-inspired optimization technique is proposed to compete with other optimizers. The main idea behind the proposed optimizer is inspired from the cooperative behaviors of one of the most intelligent birds, Harris' Hawks, in hunting escaping preys (rabbits in most cases) [37]. For this purpose, a new mathematical model is developed in this paper. Then, a stochastic metaheuristic is designed based on the proposed mathematical model to tackle various optimization problems. It should be noted that the name Harris's hawk and a similar inspiration have been used in [38], in which the authors modified the mathematical model of Grey Wolf Optimizer (MOGWO and GWO) and used it to solve multi-objective optimization problems. There were no new mathematical equations and the algorithm was developed completely based on MOGWO and GWO. In this work, however, we proposed new mathematical models to mimic all the stages of hunts used by Harris's hawks and solve single-objective optimization problems efficiently.

The rest of this research is organized as follows. Section 2 represents the background inspiration and info about the cooperative life of Harris' hawks. Section 3 represents the mathematical model and computational procedures of the HHO algorithm. The results of HHO in solving different benchmark and real-world case studies are presented in Section 4. Section 5 discusses the results. Finally, Section 6 concludes the work with some useful perspectives.

2. Background

In 1997, Louis Lefebvre proposed an approach to measure the avian "IQ" based on the observed innovations in feeding behaviors [39]. Based on his studies [39–42], the hawks can be listed amongst the most intelligent birds in nature. The Harris' hawk (*Parabuteo unicinctus*) is a well-known bird of prey that



Fig. 2. Harris's hawk.

survives in somewhat steady groups found in southern half of Arizona, USA [37]. Harmonized foraging involving several animals for catching and then, sharing the slain animal has been persuasively observed for only particular mammalian carnivores. The Harris's hawk is distinguished because of its unique cooperative foraging activities together with other family members living in the same stable group while other raptors usually attack to discover and catch a quarry, alone. This avian desert predator shows evolved innovative team chasing capabilities in tracing, encircling, flushing out, and eventually attacking the potential quarry. These smart birds can organize dinner parties consisting of several individuals in the non-breeding season. They are known as truly cooperative predators in the raptor realm. As reported by Bednarz [37] in 1998, they begin the team mission at morning twilight, with leaving the rest roosts and often perching on giant trees or power poles inside their home realm. They know their family members and try to be aware of their moves during the attack. When assembled and party gets started, some hawks one after the other make short tours and then, land on rather high perches. In this manner, the hawks occasionally will perform a "leapfrog" motion all over the target site and they rejoin and split several times to actively search for the covered animal, which is usually a rabbit.¹

The main tactic of Harris' hawks to capture a prey is "surprise pounce", which is also known as "seven kills" strategy. In this intelligent strategy, several hawks try to cooperatively attack from different directions and simultaneously converge on a detected escaping rabbit outside the cover. The attack may rapidly be completed by capturing the surprised prey in few seconds, but occasionally, regarding the escaping capabilities and behaviors of the prey, the seven kills may include multiple, short-length, quick dives nearby the prey during several minutes. Harris' hawks can demonstrate a variety of chasing styles dependent on the dynamic nature of circumstances and escaping patterns of a prey. A switching tactic occurs when the best hawk (leader) stoops at the prey and get lost, and the chase will be continued by one of the party members. These switching activities can be observed in different situations because they are beneficial for confusing the escaping rabbit. The main advantage of these cooperative tactics is that the Harris' hawks can pursue the detected rabbit to exhaustion, which increases its vulnerability. Moreover, by perplexing the escaping prey, it cannot recover its defensive capabilities and finally, it cannot escape from the confronted team besiege since one of the hawks, which is often the most powerful and experienced one, effortlessly captures the tired rabbit and shares it with other party members. Harris' hawks and their main behaviors can be seen in nature, as captured in Fig. 2.

¹ Interested readers can refer to the following documentary videos: (a) <https://bit.ly/2Qew2qN>, (b) <https://bit.ly/2qsh8Cl>, (c) <https://bit.ly/2P7OMvH>, (d) <https://bit.ly/2DosJdS>.

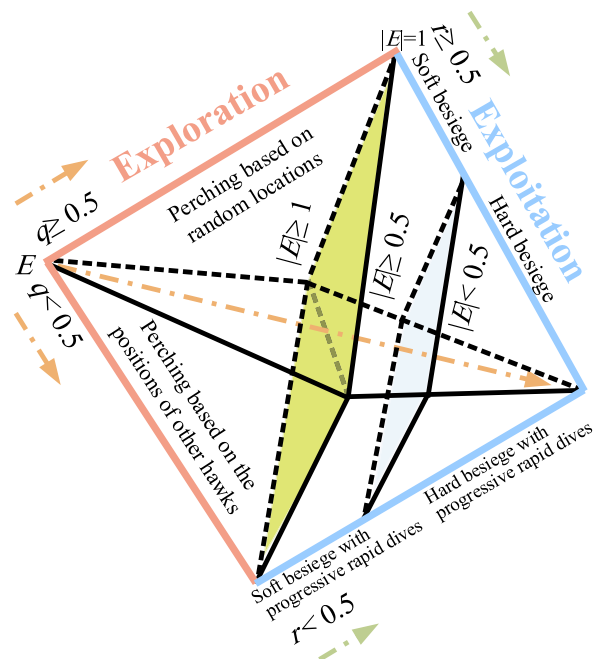


Fig. 3. Different phases of HHO.

3. Harris hawks optimization (HHO)

In this section, we model the exploratory and exploitative phases of the proposed HHO inspired by the exploring a prey, surprise pounce, and different attacking strategies of Harris hawks. HHO is a population-based, gradient-free optimization technique; hence, it can be applied to any optimization problem subject to a proper formulation. Fig. 3 shows all phases of HHO, which are described in the next subsections.

3.1. Exploration phase

In this part, the exploration mechanism of HHO is proposed. If we consider the nature of Harris' hawks, they can track and detect the prey by their powerful eyes, but occasionally the prey cannot be seen easily. Hence, the hawks wait, observe, and monitor the desert site to detect a prey maybe after several hours. In HHO, the Harris' hawks are the candidate solutions and the best candidate solution in each step is considered as the intended prey or nearly the optimum. In HHO, the Harris' hawks perch randomly on some locations and wait to detect a prey based on two strategies. If we consider an equal chance q for each perching strategy, they

perch based on the positions of other family members (to be close enough to them when attacking) and the rabbit, which is modeled in Eq. (1) for the condition of $q < 0.5$, or perch on random tall trees (random locations inside the group's home range), which is modeled in Eq. (1) for condition of $q \geq 0.5$.

$$X(t+1) = \begin{cases} X_{rand}(t) - r_1 |X_{rand}(t) - 2r_2 X(t)| & q \geq 0.5 \\ (X_{rabbit}(t) - X_m(t)) - r_3(LB + r_4(UB - LB)) & q < 0.5 \end{cases} \quad (1)$$

where $X(t+1)$ is the position vector of hawks in the next iteration t , $X_{rabbit}(t)$ is the position of rabbit, $X(t)$ is the current position vector of hawks, r_1, r_2, r_3, r_4 , and q are random numbers inside $(0,1)$, which are updated in each iteration, LB and UB show the upper and lower bounds of variables, $X_{rand}(t)$ is a randomly selected hawk from the current population, and X_m is the average position of the current population of hawks.

We proposed a simple model to generate random locations inside the group's home range (LB, UB). The first rule generates solutions based on a random location and other hawks. In second rule of Eq. (1), we have the difference of the location of best so far and the average position of the group plus a randomly-scaled component based on range of variables, while r_3 is a scaling coefficient to further increase the random nature of rule once r_4 takes close values to 1 and similar distribution patterns may occur. In this rule, we add a randomly scaled movement length to the LB . Then, we considered a random scaling coefficient for the component to provide more diversification trends and explore different regions of the feature space. It is possible to construct different updating rules, but we utilized the simplest rule, which is able to mimic the behaviors of hawks. The average position of hawks is attained using Eq. (2):

$$X_m(t) = \frac{1}{N} \sum_{i=1}^N X_i(t) \quad (2)$$

where $X_i(t)$ indicates the location of each hawk in iteration t and N denotes the total number of hawks. It is possible to obtain the average location in different ways, but we utilized the simplest rule.

3.2. Transition from exploration to exploitation

The HHO algorithm can transfer from exploration to exploitation and then, change between different exploitative behaviors based on the escaping energy of the prey. The energy of a prey decreases considerably during the escaping behavior. To model this fact, the energy of a prey is modeled as:

$$E = 2E_0(1 - \frac{t}{T}) \quad (3)$$

where E indicates the escaping energy of the prey, T is the maximum number of iterations, and E_0 is the initial state of its energy. In HHO, E_0 randomly changes inside the interval $(-1, 1)$ at each iteration. When the value of E_0 decreases from 0 to -1 , the rabbit is physically flagging, whilst when the value of E_0 increases from 0 to 1, it means that the rabbit is strengthening. The dynamic escaping energy E has a decreasing trend during the iterations. When the escaping energy $|E| \geq 1$, the hawks search different regions to explore a rabbit location, hence, the HHO performs the exploration phase, and when $|E| < 1$, the algorithm try to exploit the neighborhood of the solutions during the exploitation steps. In short, exploration happens when $|E| \geq 1$, while exploitation happens in later steps when $|E| < 1$. The time-dependent behavior of E is also demonstrated in Fig. 4.

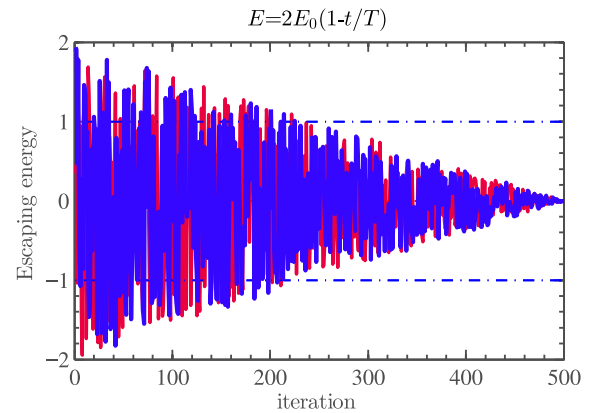


Fig. 4. Behavior of E during two runs and 500 iterations.

3.3. Exploitation phase

In this phase, the Harris' hawks perform the surprise pounce (seven kills as called in [37]) by attacking the intended prey detected in the previous phase. However, preys often attempt to escape from dangerous situations. Hence, different chasing styles occur in real situations. According to the escaping behaviors of the prey and chasing strategies of the Harris' hawks, four possible strategies are proposed in the HHO to model the attacking stage.

The preys always try to escape from threatening situations. Suppose that r is the chance of a prey in successfully escaping ($r < 0.5$) or not successfully escaping ($r \geq 0.5$) before surprise pounce. Whatever the prey does, the hawks will perform a hard or soft besiege to catch the prey. It means that they will encircle the prey from different directions softly or hard depending on the retained energy of the prey. In real situations, the hawks get closer and closer to the intended prey to increase their chances in cooperatively killing the rabbit by performing the surprise pounce. After several minutes, the escaping prey will lose more and more energy; then, the hawks intensify the besiege process to effortlessly catch the exhausted prey. To model this strategy and enable the HHO to switch between soft and hard besiege processes, the E parameter is utilized.

In this regard, when $|E| \geq 0.5$, the soft besiege happens, and when $|E| < 0.5$, the hard besiege occurs.

3.3.1. Soft besiege

When $r \geq 0.5$ and $|E| \geq 0.5$, the rabbit still has enough energy, and try to escape by some random misleading jumps but finally it cannot. During these attempts, the Harris' hawks encircle it softly to make the rabbit more exhausted and then perform the surprise pounce. This behavior is modeled by the following rules:

$$X(t+1) = \Delta X(t) - E |J X_{rabbit}(t) - X(t)| \quad (4)$$

$$\Delta X(t) = X_{rabbit}(t) - X(t) \quad (5)$$

where $\Delta X(t)$ is the difference between the position vector of the rabbit and the current location in iteration t , r_5 is a random number inside $(0,1)$, and $J = 2(1 - r_5)$ represents the random jump strength of the rabbit throughout the escaping procedure. The J value changes randomly in each iteration to simulate the nature of rabbit motions.

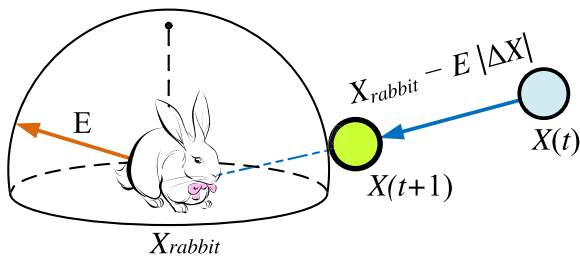


Fig. 5. Example of overall vectors in the case of hard besiege.

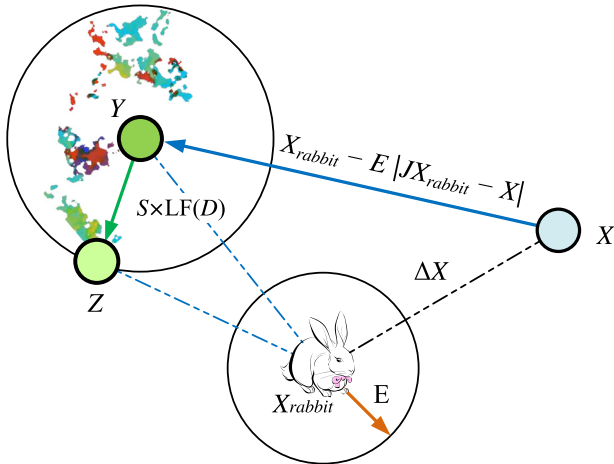


Fig. 6. Example of overall vectors in the case of soft besiege with progressive rapid dives.

3.3.2. Hard besiege

When $r \geq 0.5$ and $|E| < 0.5$, the prey is so exhausted and it has a low escaping energy. In addition, the Harris' hawks hardly encircle the intended prey to finally perform the surprise pounce. In this situation, the current positions are updated using Eq. (6):

$$X(t + 1) = X_{rabbit}(t) - E |\Delta X(t)| \quad (6)$$

A simple example of this step with one hawk is depicted in Fig. 5.

3.3.3. Soft besiege with progressive rapid dives

When still $|E| \geq 0.5$ but $r < 0.5$, the rabbit has enough energy to successfully escape and still a soft besiege is constructed before the surprise pounce. This procedure is more intelligent than the previous case.

To mathematically model the escaping patterns of the prey and *leapfrog movements* (as called in [37]), the levy flight (LF) concept is utilized in the HHO algorithm. The LF is utilized to mimic the real zigzag deceptive motions of preys (particularly rabbits) during escaping phase and irregular, abrupt, and rapid dives of hawks around the escaping prey. Actually, hawks perform several team rapid dives around the rabbit and try to progressively correct their location and directions with regard to the deceptive motions of prey. This mechanism is also supported by real observations in other competitive situations in nature. It has been confirmed that LF-based activities are the optimal searching tactics for foragers/predators in non-destructive foraging conditions [43,44]. In addition, it has been detected the LF-based patterns can be detected in the chasing activities of animals like monkeys and sharks [45–48]. Hence, the LF-based motions were utilized within this phase of HHO technique.

Inspired by real behaviors of hawks, we supposed that they can progressively select the best possible dive toward the prey

when they wish to catch the prey in the competitive situations. Therefore, to perform a soft besiege, we supposed that the hawks can evaluate (decide) their next move based on the following rule in Eq. (7):

$$Y = X_{rabbit}(t) - E |JX_{rabbit}(t) - X(t)| \quad (7)$$

Then, they compare the possible result of such a movement to the previous dive to detect that will it be a good dive or not. If it was not reasonable (when they see that the prey is performing more deceptive motions), they also start to perform irregular, abrupt, and rapid dives when approaching the rabbit. We supposed that they will dive based on the LF-based patterns using the following rule:

$$Z = Y + S \times LF(D) \quad (8)$$

where D is the dimension of problem and S is a random vector by size $1 \times D$ and LF is the levy flight function, which is calculated using Eq. (9) [49]:

$$LF(x) = 0.01 \times \frac{u \times \sigma}{|v|^{\frac{1}{\beta}}}, \sigma = \left(\frac{\Gamma(1 + \beta) \times \sin(\frac{\pi \beta}{2})}{\Gamma(\frac{1+\beta}{2}) \times \beta \times 2^{(\frac{\beta-1}{2})}} \right)^{\frac{1}{\beta}} \quad (9)$$

where u, v are random values inside $(0,1)$, β is a default constant set to 1.5.

Hence, the final strategy for updating the positions of hawks in the soft besiege phase can be performed by Eq. (10):

$$X(t + 1) = \begin{cases} Y & \text{if } F(Y) < F(X(t)) \\ Z & \text{if } F(Z) < F(X(t)) \end{cases} \quad (10)$$

where Y and Z are obtained using Eqs. (7) and (8).

A simple illustration of this step for one hawk is demonstrated in Fig. 6. Note that the position history of LF-based leapfrog movement patterns during some iterations are also recorded and shown in this illustration. The colored dots are the location footprints of LF-based patterns in one trial and then, the HHO reaches to the location Z . In each step, only the better position Y or Z will be selected as the next location. This strategy is applied to all search agents.

3.3.4. Hard besiege with progressive rapid dives

When $|E| < 0.5$ and $r < 0.5$, the rabbit has not enough energy to escape and a hard besiege is constructed before the surprise pounce to catch and kill the prey. The situation of this step in the prey side is similar to that in the soft besiege, but this time, the hawks try to decrease the distance of their average location with the escaping prey. Therefore, the following rule is performed in hard besiege condition:

$$X(t + 1) = \begin{cases} Y & \text{if } F(Y) < F(X(t)) \\ Z & \text{if } F(Z) < F(X(t)) \end{cases} \quad (11)$$

where Y and Z are obtained using new rules in Eqs. (12) and (13).

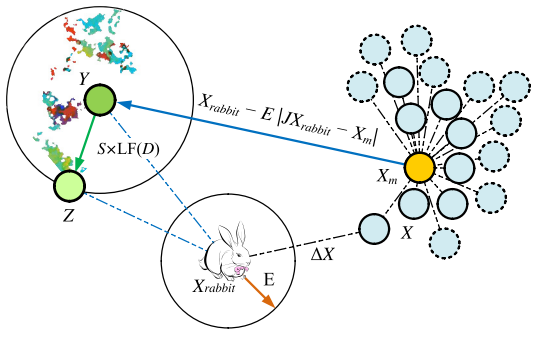
$$Y = X_{rabbit}(t) - E |JX_{rabbit}(t) - X_m(t)| \quad (12)$$

$$Z = Y + S \times LF(D) \quad (13)$$

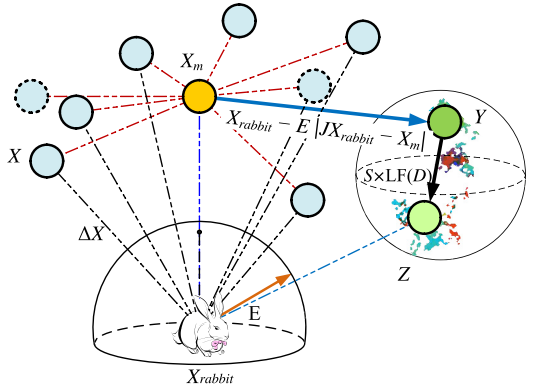
where $X_m(t)$ is obtained using Eq. (2). A simple example of this step is demonstrated in Fig. 7. Note that the colored dots are the location footprints of LF-based patterns in one trial and only Y or Z will be the next location for the new iteration.

3.4. Pseudocode of HHO

The pseudocode of the proposed HHO algorithm is reported in Algorithm 1.



(a) The process in 2D space



(b) The process in 3D space

Fig. 7. Example of overall vectors in the case of hard besiege with progressive rapid dives in 2D and 3D space.

3.5. Computational complexity

Note that the computational complexity of the HHO mainly depends on three processes: initialization, fitness evaluation, and updating of hawks. Note that with N hawks, the computational complexity of the initialization process is $O(N)$. The computational complexity of the updating mechanism is $O(T \times N) + O(T \times N \times D)$, which is composed of searching for the best location and updating the location vector of all hawks, where T is the maximum number of iterations and D is the dimension of specific problems. Therefore, computational complexity of HHO is $O(N \times (T + TD + 1))$.

Algorithm 1 Pseudo-code of HHO algorithm

```

Inputs: The population size  $N$  and maximum number of iterations  $T$ 
Outputs: The location of rabbit and its fitness value
Initialize the random population  $X_i (i = 1, 2, \dots, N)$ 
while (stopping condition is not met) do
    Calculate the fitness values of hawks
    Set  $X_{rabbit}$  as the location of rabbit (best location)
    for (each hawk ( $X_i$ )) do
        Update the initial energy  $E_0$  and jump strength  $J$       ▷
         $E_0 = 2\text{rand}() - 1, J = 2(1 - \text{rand}())$ 
        Update the  $E$  using Eq. (3)                                ▷ Exploration phase
        if ( $|E| \geq 1$ ) then                                     ▷ Exploration phase
            Update the location vector using Eq. (1)
        if ( $|E| < 1$ ) then                                    ▷ Exploitation phase
            if ( $r \geq 0.5$  and  $|E| \geq 0.5$ ) then          ▷ Soft besiege
                Update the location vector using Eq. (4)
            else if ( $r \geq 0.5$  and  $|E| < 0.5$ ) then          ▷ Hard besiege
                Update the location vector using Eq. (6)
            else if ( $r < 0.5$  and  $|E| \geq 0.5$ ) then          ▷ Soft besiege
                with progressive rapid dives
                Update the location vector using Eq. (10)
            else if ( $r < 0.5$  and  $|E| < 0.5$ ) then          ▷ Hard besiege
                with progressive rapid dives
                Update the location vector using Eq. (11)
        Return  $X_{rabbit}$ 
```

4. Experimental results and discussions

4.1. Benchmark set and compared algorithms

In order to investigate the efficacy of the proposed HHO optimizer, a well-studied set of diverse benchmark functions are selected from literature [50,51]. This benchmark set covers three main groups of benchmark landscapes: unimodal (UM), multimodal (MM), and composition (CM). The UM functions (F1–F7) with unique global best can reveal the exploitative (intensification) capacities of different optimizers, while the MM functions (F8–F23) can disclose the exploration (diversification) and LO avoidance potentials of algorithms. The mathematical formulation and characteristics of UM and MM problems are shown in Tables 16–18 in Appendix A. The third group problems (F24–F29) are selected from IEEE CEC 2005 competition [52] and covers hybrid composite, rotated and shifted MM test cases. These CM cases are also utilized in many papers and can expose the performance of utilized optimizers in well balancing the exploration

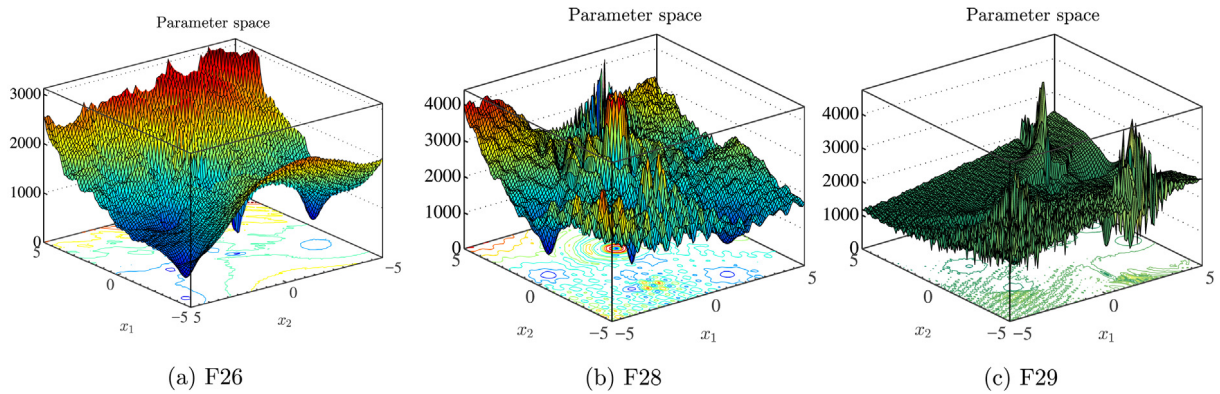


Fig. 8. Demonstration of composition test functions.

Table 1

The parameter settings.

Algorithm	Parameter	Value
DE	Scaling factor	0.5
	Crossover probability	0.5
PSO	Topology fully connected	
	Inertia factor	0.3
	c_1	1
TLBO	c_2	1
	Teaching factor T	1, 2
	Convergence constant a	[2 0]
GWO	Convergence constant a	[-2 -1]
	Spiral factor b	1
MFO	Discovery rate of alien solutions p_a	0.25
	Q_{min} Frequency minimum	0
	Q_{max} Frequency maximum	2
	A Loudness	0.5
CS	r Pulse rate	0.5
	α	0.5
	β	0.2
BA	γ	1
	Probability switch p	0.8
	Habitat modification probability	1
FPA	Immigration probability limits	[0, 1]
	Step size	1
	Max immigration (I) and Max emigration (E)	1
BBO	Mutation probability	0.005

and exploitation inclinations and escaping from LO in dealing with challenging problems. Details of the CM test problems are also reported in Table 19 in Appendix A. Fig. 8 demonstrates three of composition test problems.

The results and performance of the proposed HHO is compared with other well-established optimization techniques such as the GA [22], BBO [22], DE [22], PSO [22], CS [34], TLBO [29], BA/BAT [53], FPA [54], FA [55], GWO [56], and MFO [57] algorithms based on the best, worst, standard deviation (STD) and average of the results (AVG). These algorithms cover both recently proposed techniques such as MFO, GWO, CS, TLBO, BAT, FPA, and FA and also, relatively the most utilized optimizers in the field like the GA, DE, PSO, and BBO algorithms.

As recommended by Derrac et al. [58], the non-parametric Wilcoxon statistical test with 5% degree of significance is also performed along with experimental assessments to detect the significant differences between the attained results of different techniques.

4.2. Experimental setup

All algorithms were implemented under Matlab 7.10 (R2010a) on a computer with a Windows 7 64-bit professional and 64 GB RAM. The swarm size and maximum iterations of all optimizers are set to 30 and 500, respectively. All results are recorded and compared based on the average performance of optimizers over 30 independent runs.

The settings of GA, PSO, DE and BBO algorithms are same with those set by Dan Simon in the original work of BBO [22], while for the BA [53], FA [59], TLBO [29], GWO [56], FPA [54], CS [34], and MFO [57], the parameters are same with the recommended settings in the original works. The used parameters are also reported in Table 1.

4.3. Qualitative results of HHO

The qualitative results of HHO for several standard unimodal and multimodal test problems are demonstrated in Figs. 9–11. These results include four well-known metrics: search history, the trajectory of the first hawk, average fitness of population, and convergence behavior. In addition, the escaping energy of

the rabbit is also monitored during iterations. The search history diagram reveals the history of those positions visited by artificial hawks during iterations. The map of the trajectory of the first hawk monitors how the first variable of the first hawk varies during the steps of the process. The average fitness of hawks monitors how the average fitness of whole population varies during the process of optimization. The convergence metric also reveals how the fitness value of the rabbit (best solution) varies during the optimization. Note that the diagram of escaping energy demonstrates how the energy of rabbit varies during the simulation.

From the history of sampled locations in Figs. 9–11, it can be observed that the HHO reveals a similar pattern in dealing with different cases, in which the hawks attempts to initially boost the diversification and explore the favorable areas of solution space and then exploit the vicinity of the best locations. The diagram of trajectories can help us to comprehend the searching behavior of the foremost hawk (as a representative of the rest of hawks). By this metric, we can check if the foremost hawk faces abrupt changes during the early phases and gradual variations in the concluding steps. Referring to Van Den Bergh and Engelbrecht [60], these activities can guarantee that a P-metaheuristic finally converges to a position and exploit the target region.

As per trajectories in Figs. 9–11, we see that the foremost hawk start the searching procedure with sudden movements. The amplitude of these variations covers more than 50% of the solution space. This observation can disclose the exploration propensities of the proposed HHO. As times passes, the amplitude of these fluctuations gradually decreases. This point guarantees the transition of HHO from exploratory trends to exploitative steps. Eventually, the motion pattern of the first hawk becomes very stable which shows that the HHO is exploiting the promising regions during the concluding steps. By monitoring the average fitness of the population, the next measure, we can notice the reduction patterns in fitness values when the HHO enriches the excellence of the randomized candidate hawks. Based on the diagrams demonstrated in Figs. 9–11, the HHO can enhance the quality of all hawks during half of the iterations and there is an accelerating decreasing pattern in all curves. Again, the amplitude of variations of fitness results decreases by more iteration. Hence, the HHO can dynamically focus on more promising areas during iterations. According to convergence curves in Fig. Figs. 9–11, which shows the average fitness of best hawk found so far, we can detect accelerated decreasing patterns in all curves, especially after half of the iteration. We can also detect the estimated moment that the HHO shift from exploration to exploitation. In this regard, it is observed that the HHO can reveal an accelerated convergence trend.

4.4. Scalability analysis

In this section, a scalability assessment is utilized to investigate the impact of dimension on the results of HHO. This test has been utilized in the previous studies and it can reveal the impact of dimensions on the quality of solutions for the HHO optimizer to recognize its efficacy not only for problems with lower dimensions but also for higher dimension tasks. In addition, it reveals how a P-metaheuristic can preserve its searching advantages in higher dimensions. For this experiment, the HHO is utilized to tackle the scalable UM and MM F1–F13 test cases with 30, 100, 500, and 1000 dimensions. The average error AVG and STD of the attained results of all optimizers over 30 independent runs and 500 iterations are recorded and compared for each dimension. Table 2 reveals the results of HHO versus other methods in dealing with F1–F13 problems with different dimensions. The scalability results for all techniques are also illustrated in Fig. 12.

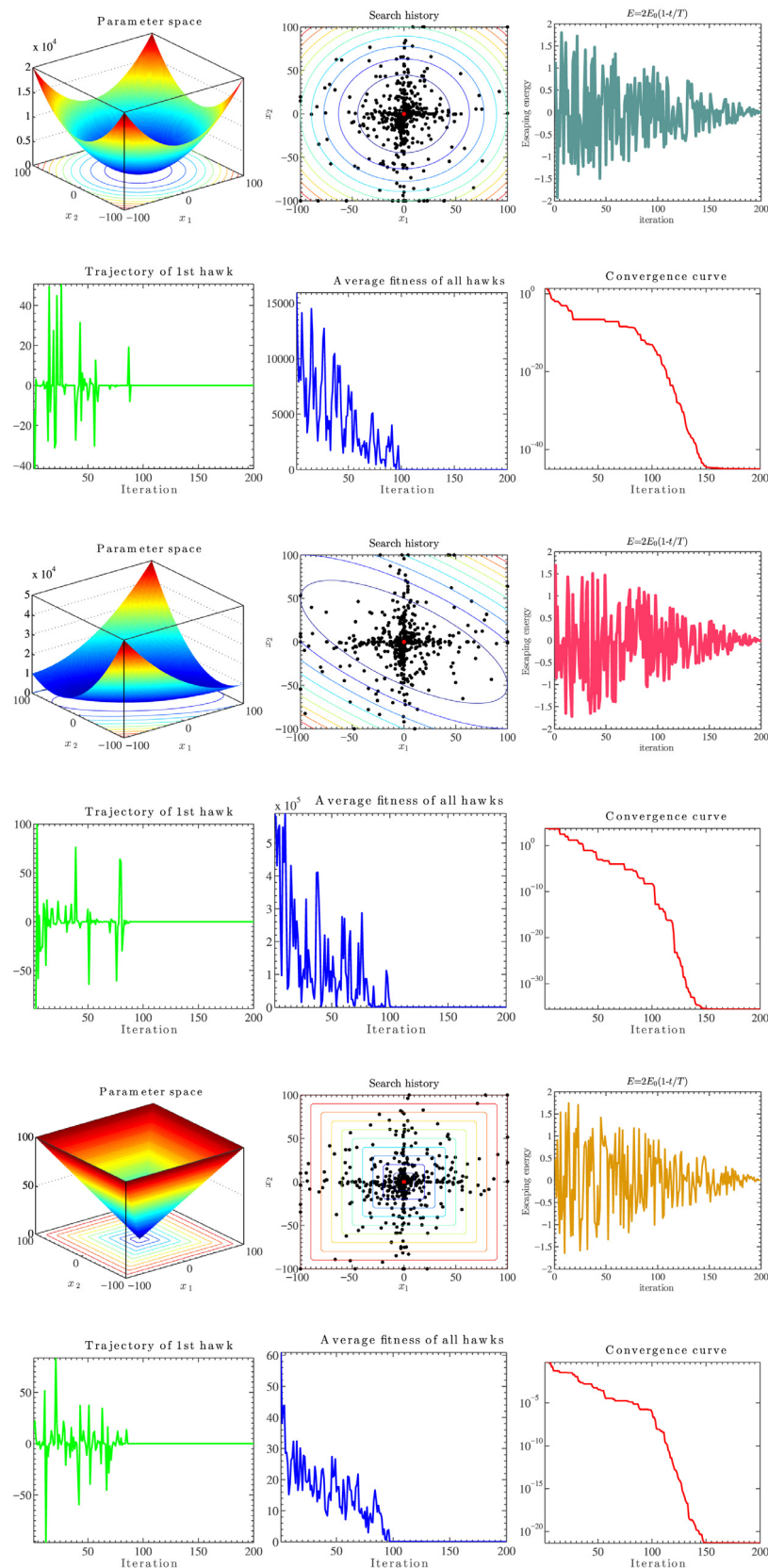
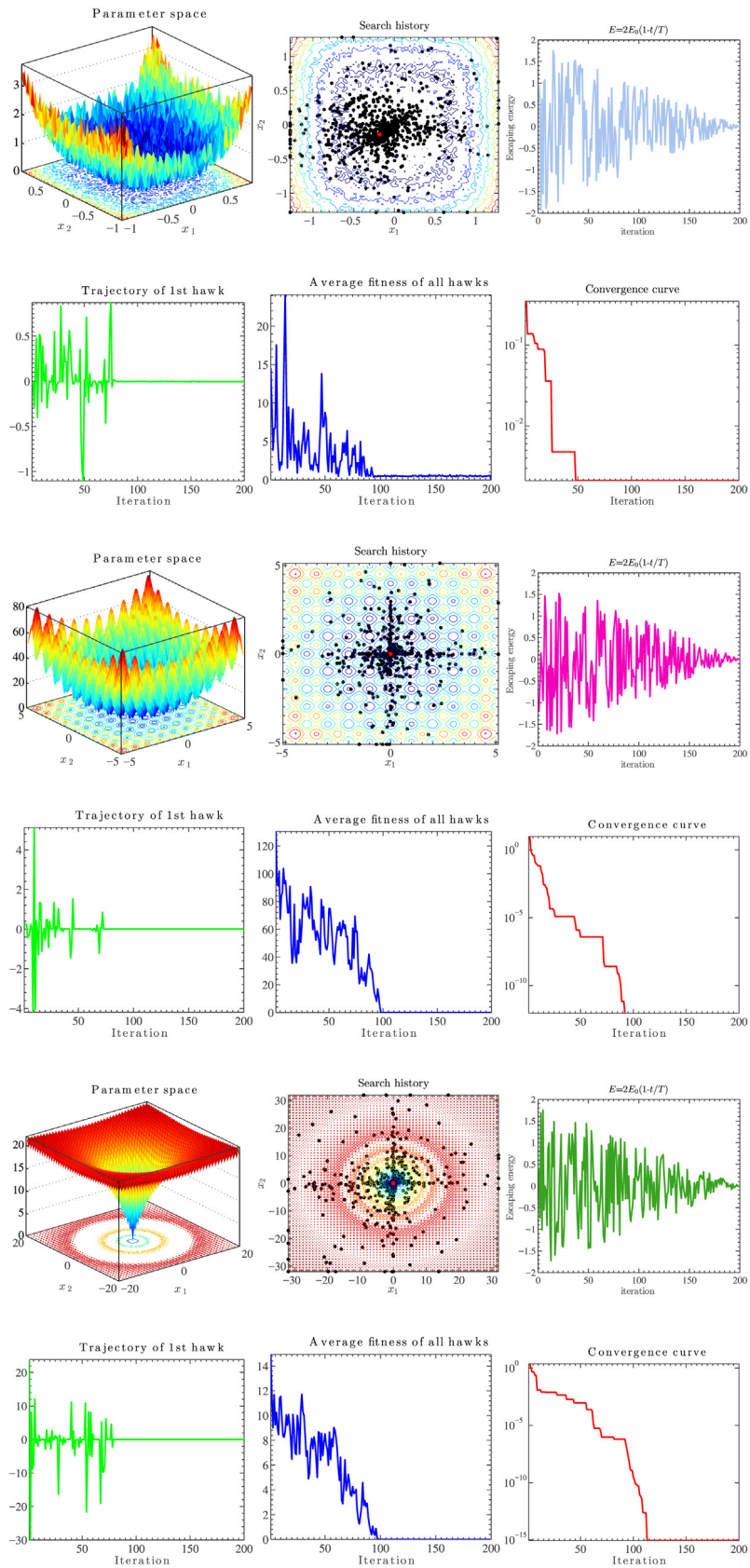


Fig. 9. Qualitative results for unimodal F1, F3, and F4 problems.

**Fig. 10.** Qualitative results for F7, F9, and F10 problems.

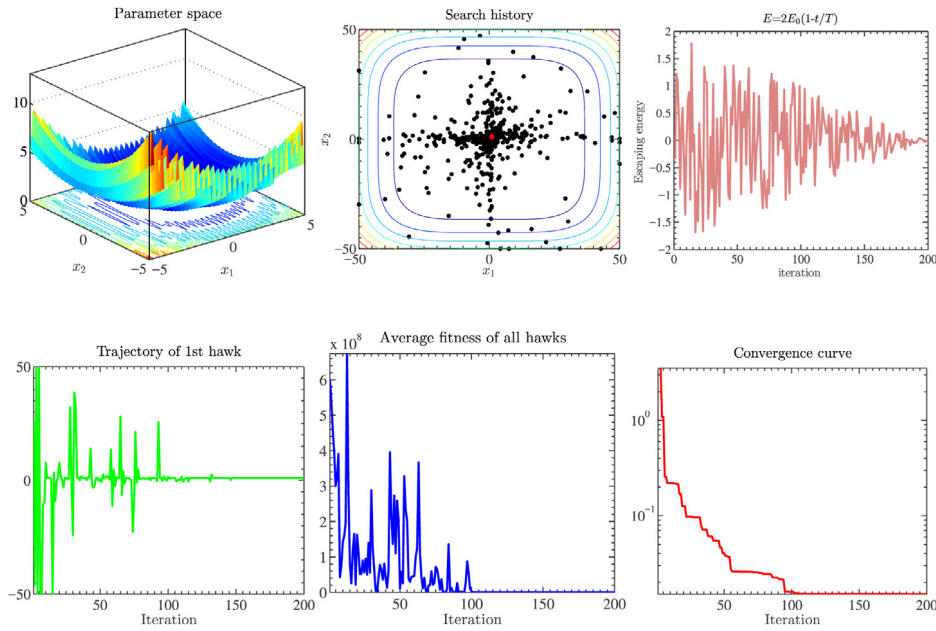


Fig. 11. Qualitative results for F13 problem.

Table 2
Results of HHO for different dimensions of scalable F1–F13 problems.

Problem/D	Metric	30	100	500	1000
F1	AVG	3.95E–97	1.91E–94	1.46E–92	1.06E–94
	STD	1.72E–96	8.66E–94	8.01E–92	4.97E–94
F2	AVG	1.56E–51	9.98E–52	7.87E–49	2.52E–50
	STD	6.98E–51	2.66E–51	3.11E–48	5.02E–50
F3	AVG	1.92E–63	1.84E–59	6.54E–37	1.79E–17
	STD	1.05E–62	1.01E–58	3.58E–36	9.81E–17
F4	AVG	1.02E–47	8.76E–47	1.29E–47	1.43E–46
	STD	5.01E–47	4.79E–46	4.11E–47	7.74E–46
F5	AVG	1.32E–02	2.36E–02	3.10E–01	5.73E–01
	STD	1.87E–02	2.99E–02	3.73E–01	1.40E+00
F6	AVG	1.15E–04	5.12E–04	2.94E–03	3.61E–03
	STD	1.56E–04	6.77E–04	3.98E–03	5.38E–03
F7	AVG	1.40E–04	1.85E–04	2.51E–04	1.41E–04
	STD	1.07E–04	4.06E–04	2.43E–04	1.63E–04
F8	AVG	–1.25E+04	–4.19E+04	–2.09E+05	–4.19E+05
	STD	1.47E+02	2.82E+00	2.84E+01	1.03E+02
F9	AVG	0.00E+00	0.00E+00	0.00E+00	0.00E+00
	STD	0.00E+00	0.00E+00	0.00E+00	0.00E+00
F10	AVG	8.88E–16	8.88E–16	8.88E–16	8.88E–16
	STD	4.01E–31	4.01E–31	4.01E–31	4.01E–31
F11	AVG	0.00E+00	0.00E+00	0.00E+00	0.00E+00
	STD	0.00E+00	0.00E+00	0.00E+00	0.00E+00
F12	AVG	7.35E–06	4.23E–06	1.41E–06	1.02E–06
	STD	1.19E–05	5.25E–06	1.48E–06	1.16E–06
F13	AVG	1.57E–04	9.13E–05	3.44E–04	8.41E–04
	STD	2.15E–04	1.26E–04	4.75E–04	1.18E–03

Note that the detailed results of all techniques are reported in the next parts.

As it can be seen in Table 2, the HHO can expose excellent results in all dimensions and its performance remains consistently superior when realizing cases with many variables. As per curves in Fig. 12, it is observed that the optimality of results and the performance of other methods significantly degrade by increasing the dimensions. This reveals that HHO is capable of maintaining a good balance between the exploratory and exploitative tendencies on problems with many variables.

4.5. Quantitative results of HHO and discussion

In this section, the results of HHO are compared with those of other optimizers for different dimensions of F1–F13 test problems in addition to the F14–F29 MM and CM test cases. Note that the results are presented for 30, 100, 500, and 1000 dimensions of the scalable F1–F13 problems. Tables 3–6 show the obtained results for HHO versus other competitors in dealing with scalable functions. Table 8 also reveals the performance of algorithms in dealing with F14–F29 test problems. In order to investigate the significant differences between the results of proposed HHO

Table 3

Results of benchmark functions (F1–F13), with 30 dimensions.

Benchmark	HHO	GA	PSO	BBO	FPA	GWO	BAT	FA	CS	MFO	TLBO	DE	
F1	AVG STD	3.95E–97 1.72E–96	1.03E+03 5.79E+02	1.83E+04 3.01E+03	7.59E+01 2.75E+01	2.01E+03 5.60E+02	1.18E–27 1.47E–27	6.59E+04 7.51E+03	7.11E–03 3.21E–03	9.06E–04 4.55E–04	1.01E+03 3.05E+03	2.17E–89 3.14E–89	1.33E–03 5.92E–04
F2	AVG STD	1.56E–51 6.98E–51	2.47E+01 1.35E+03	3.58E+02 7.45E–03	1.36E–03 5.55E+00	3.22E+01 5.60E–17	9.71E–17 1.30E+09	2.71E+08 1.84E–01	4.34E–01 1.49E–01	3.19E+01 2.79E–02	2.77E–45 2.06E+01	6.83E–03 3.11E–45	2.06E–03
F3	AVG STD	1.92E–63 1.05E–62	2.65E+04 3.44E+03	4.05E+04 8.21E+03	1.21E+04 2.69E+03	1.41E+03 5.59E+02	5.12E–05 2.03E–04	1.38E+05 4.72E+04	1.66E+03 6.72E+02	2.10E–01 5.69E–02	2.43E+04 1.41E+04	3.91E–18 8.04E–18	3.97E+04 5.37E+03
F4	AVG STD	1.02E–47 5.01E–47	5.17E+01 1.05E+01	4.39E+01 3.64E+00	3.02E+01 2.77E+00	2.38E+01 1.94E–06	1.24E–06 2.95E+00	8.51E+01 4.75E+00	1.11E–01 1.94E–02	9.65E–02 7.06E+00	7.00E+01 1.47E–36	1.68E–36 2.37E+00	1.15E+01
F5	AVG STD	1.32E–02 1.87E–02	1.95E+04 1.31E+04	1.96E+07 6.25E+06	1.82E+03 9.40E+02	3.17E+05 1.75E+05	2.70E+01 7.78E–01	2.10E+08 4.17E+07	7.97E+01 7.39E+01	2.76E+01 4.51E–01	7.35E+03 2.26E+04	2.54E+01 4.26E–01	1.06E+02 1.01E+02
F6	AVG STD	1.15E–04 1.56E–04	9.01E+02 2.84E+02	1.87E+04 2.92E+03	6.71E+01 2.20E+01	1.70E+03 3.13E+02	8.44E–01 3.18E–01	6.69E+04 5.87E+03	6.94E–03 1.30E–03	3.13E–03 3.61E–03	2.68E+03 5.84E+03	3.29E–05 8.65E–05	1.44E–03 5.38E–04
F7	AVG STD	1.40E–04 1.07E–04	1.91E–01 1.50E–01	1.07E+01 3.05E+00	2.91E–03 1.83E–03	3.41E–01 1.10E–01	1.70E–03 1.06E–03	4.57E+01 7.82E+00	6.62E–02 4.23E–02	7.29E–02 2.21E–02	4.50E+00 9.21E+00	1.16E–03 3.63E–04	5.24E–02 1.37E–02
F8	AVG STD	–1.25E+04 1.47E+02	–1.26E+04 4.51E+00	–3.86E+03 2.49E+02	–1.24E+04 3.50E+01	–6.45E+03 3.03E+02	–5.97E+03 7.10E+02	–2.33E+03 2.96E+02	–5.85E+03 1.16E+03	–5.19E+19 1.76E+20	–8.48E+03 7.98E+02	–7.76E+03 1.04E+03	–6.82E+03 3.94E+02
F9	AVG STD	0.00E+00 0.00E+00	9.04E+00 4.58E+00	0.00E+00 1.95E+01	2.87E+02 0.00E+00	1.82E+02 1.24E+01	2.19E+00 3.69E+00	1.92E+02 3.56E+01	3.82E+01 1.12E+01	1.51E+01 1.25E+00	1.59E+02 3.21E+01	1.40E+01 5.45E+00	1.58E+02 1.17E+01
F10	AVG STD	8.88E–16 4.01E–31	1.36E+01 1.51E+00	1.75E+01 3.67E–01	2.13E+00 3.53E–01	7.14E+00 1.08E+00	1.03E–13 1.70E–14	1.92E+01 2.43E–01	4.58E–02 1.20E–02	3.29E–02 4.95E+00	1.74E+01 7.93E–03	6.45E–15 1.79E–15	1.21E–02 3.30E–03
F11	AVG STD	0.00E+00 0.00E+00	1.01E+01 2.43E+00	1.70E+02 3.17E+01	1.46E+00 1.69E–01	1.73E+01 3.63E+00	4.76E–03 8.57E–03	6.01E+02 5.50E+01	4.23E–03 1.29E–03	4.29E–05 2.00E–05	3.10E+01 5.94E+01	0.00E+00 0.00E+00	3.52E–02 7.20E–02
F12	AVG STD	2.08E–06 1.19E–05	4.77E+00 1.56E+00	1.51E+07 9.88E+06	6.68E–01 2.62E–01	3.05E+02 1.04E+03	4.83E–02 2.12E–02	4.71E+08 1.54E+08	3.13E–04 1.76E–04	5.57E–05 4.96E–05	2.46E+02 1.21E+03	7.35E–06 7.45E–06	2.25E–03 1.70E–03
F13	AVG STD	1.57E–04 2.15E–04	1.52E+01 4.52E+00	5.73E+07 2.68E+07	1.82E+00 3.41E–01	9.59E+04 1.46E+05	5.96E–01 2.23E–01	9.40E+08 1.67E+08	2.08E–03 9.62E–04	8.19E–03 6.74E–03	2.73E+07 1.04E+08	7.89E–02 8.78E–02	9.12E–03 1.16E–02

Table 4

Results of benchmark functions (F1–F13), with 100 dimensions.

Benchmark	HHO	GA	PSO	BBO	FPA	GWO	BAT	FA	CS	MFO	TLBO	DE	
F1	AVG STD	1.91E–94 8.66E–94	5.41E+04 1.42E+04	1.06E+05 8.47E+03	2.85E+03 4.49E+02	1.39E+04 2.71E+03	1.59E–12 1.63E–12	2.72E+05 1.42E+04	3.05E–01 5.60E–02	3.17E–01 5.28E–02	6.20E+04 1.25E+04	3.62E–81 4.14E–81	8.26E+03 1.32E+03
F2	AVG STD	9.98E–52 2.66E–51	2.53E+02 1.41E+01	6.06E+23 2.18E+24	1.59E+01 3.74E+00	1.01E+02 9.36E+00	4.31E–08 1.46E–08	6.00E+43 1.18E+44	1.45E+01 6.73E+00	4.05E+00 3.16E–01	2.46E+02 4.48E+01	3.27E–41 2.75E–41	1.21E+02 2.33E+01
F3	AVG STD	1.84E–59 1.01E–58	2.53E+05 5.03E+04	4.22E+05 7.08E+04	1.70E+05 2.02E+04	1.89E+04 5.44E+03	4.09E+02 2.77E+02	1.43E+06 6.21E+05	4.65E+04 6.92E+03	6.88E+00 1.02E+00	2.15E+05 4.43E+04	4.33E–07 8.20E–07	5.01E+05 5.87E+04
F4	AVG STD	8.76E–47 4.79E–46	8.19E+01 3.15E+00	6.07E+01 3.05E+00	7.08E+01 4.73E+00	3.51E+01 3.37E+00	8.89E–01 9.30E–01	9.41E+01 1.49E+00	1.91E+01 2.80E–02	2.58E–01 2.13E+00	9.31E+01 6.66E–33	6.36E–33 1.00E+00	9.62E+01 5.66E–33
F5	AVG STD	2.36E–02 2.99E–02	2.37E+07 8.43E+06	2.42E+08 4.02E+07	4.47E+05 2.05E+05	4.64E+06 1.98E+06	9.79E+01 6.75E–01	1.10E+09 9.47E+07	8.46E+02 8.13E+02	1.33E+02 7.34E+00	1.44E+08 7.50E+07	9.67E+01 7.77E–01	1.99E+07 5.80E+06
F6	AVG STD	5.12E–04 6.77E–04	5.42E+04 1.09E+04	1.07E+05 9.70E+03	2.85E+03 4.07E+02	1.26E+04 2.06E+03	1.03E+01 1.05E+00	2.69E+05 1.25E+04	2.95E–01 5.34E–02	2.65E+00 3.94E–01	6.68E+04 1.46E+04	3.27E+00 6.98E–01	8.07E+03 1.64E+03
F7	AVG STD	1.85E–04 4.06E–04	2.73E+01 4.45E+01	3.41E+02 8.74E+01	1.25E+00 5.18E+00	5.84E+00 2.16E+00	7.60E–03 2.66E–03	3.01E+02 2.66E+01	5.65E–01 1.64E–01	1.21E+00 2.65E–01	2.56E+02 8.91E+01	1.50E–03 5.39E–04	1.96E+01 5.66E+00
F8	AVG STD	–4.19E+04 2.82E+00	–4.10E+04 1.14E+02	–7.33E+03 4.75E+02	–3.85E+04 2.80E+02	–1.28E+04 4.64E+02	–1.67E+04 2.62E+03	–4.07E+03 9.37E+02	–1.81E+04 3.23E+03	–2.84E+18 6.91E+18	–2.30E+04 1.98E+03	–1.71E+04 3.54E+03	–1.19E+04 5.80E+02
F9	AVG STD	0.00E+00 0.00E+00	3.39E+02 4.17E+01	1.16E+03 5.74E+01	9.11E+00 2.73E+00	8.47E+02 4.01E+01	1.03E+01 9.02E+00	7.97E+02 6.33E+01	2.36E+02 2.63E+01	1.72E+02 9.24E+00	8.65E+02 8.01E+01	1.02E+01 5.57E+01	1.03E+03 4.03E+01
F10	AVG STD	8.88E–16 4.01E–31	1.82E+01 4.35E–01	1.91E+01 4.72E–01	5.57E+00 1.14E+00	8.21E+00 5.07E–08	1.20E–07 6.50E–02	1.94E+01 2.55E–01	9.81E–01 8.58E–02	3.88E–01 8.58E–02	1.99E+01 9.10E–02	1.66E–02 9.10E–02	1.22E+01 8.31E–01
F11	AVG STD	0.00E+00 0.00E+00	5.14E+02 1.05E+02	9.49E+02 6.00E+01	2.24E+01 4.35E+00	1.19E+02 2.00E+01	4.87E–03 1.07E–02	2.47E+03 1.03E+02	1.19E–01 2.34E–02	4.56E–03 9.73E–04	5.60E+02 1.23E+02	0.00E+00 0.00E+00	7.42E+01 1.40E+01
F12	AVG STD	4.23E–06 5.25E–06	4.55E+06 8.22E+06	3.54E+08 8.75E+07	3.03E+02 1.48E+03	1.55E+05 1.74E+02	2.87E–01 2.69E+08	2.64E+09 1.32E+00	4.45E+00 2.59E+03	2.47E–02 1.45E+08	2.82E+08 1.02E+02	3.03E–02 1.28E+07	3.90E+07 1.88E+07
F13	AVG STD	9.13E–05 1.26E–04	5.26E+07 3.76E+07	8.56E+08 2.16E+08	6.82E+04 3.64E+04	2.76E+06 1.80E+06	6.87E+00 3.32E–01	5.01E+09 3.93E+08	4.50E+01 2.24E+01	5.84E+00 1.21E+00	6.68E+08 3.05E+08	5.47E+00 8.34E–01	7.19E+07 2.73E+07

versus other optimizers, Wilcoxon rank-sum test with 5% degree is carefully performed here [58]. Tables 20–24 in Appendix B show the attained p-values of the Wilcoxon rank-sum test with 5% significance. As per result in Table 3, the HHO can obtain the best results compared to other competitors on F1–F5, F7, and F9–F13 problems. The results of HHO are considerably better than other algorithms in dealing with 84.6% of these 30-dimensional functions, demonstrating the superior performance of this optimizer. According to p-values in Table 20, it is detected that the observed differences in the results are statistically meaningful for all cases. From Table 4, when we have a 100-dimensional search space, the HHO can considerably outperform other techniques and attain the best results for 92.3% of F1–F13 problems. It is observed that the results of HHO are again remarkably better than other techniques. With regard to p-values in Table 21, it is detected that the solutions of HHO are significantly better than those realized by other techniques in almost all cases. From Table 5, we see that the HHO can attain the best results in terms of AVG and STD in dealing with 12 test cases with 500 dimensions. By considering p-values in Table 22, it is recognized that the HHO can significantly

outperform other optimizers in all cases. As per results in Table 6, similarly to what we observed in lower dimensions, it is detected that the HHO has still a remarkably superior performance in dealing with F1–F13 test functions compared to GA, PSO, DE, BBO, CS, GWO, MFO, TLBO, BAT, FA, and FPA optimizers. The statistical results in Table 23 also verify the significant gap between the results of HHO and other optimizers in almost all cases. It is seen that the HHO has reached the best global optimum for F9 and F11 cases in any dimension.

In order to further check the efficacy of HHO, we recorded the running time taken by optimizers to find the solutions for F1–F13 problems with 1000 dimensions and the results are exposed in Table 7. As per results in Table 7, we detect that the HHO shows a reasonably fast and competitive performance in finding the best solutions compared to other well-established optimizers even for high dimensional unimodal and multimodal cases. Based on average running time on

Table 5

Results of benchmark functions (F1–F13), with 500 dimensions.

Benchmark	HHO	GA	PSO	BBO	FPA	GWO	BAT	FA	CS	MFO	TLBO	DE	
F1	AVG STD	1.46E−92 8.01E−92	6.06E+05 7.01E+04	6.42E+05 2.96E+04	1.60E+05 9.76E+03	8.26E+04 1.32E+04	1.42E−03 3.99E−04	1.52E+06 3.58E+04	6.30E+04 8.47E+03	6.80E+00 4.93E−01	1.15E+06 3.54E+04	2.14E−77 1.94E−77	7.43E+05 3.67E+04
F2	AVG STD	7.87E−49 3.11E−48	1.94E+03 7.03E+01	6.08E+09 1.70E+10	5.95E+02 1.70E+01	5.13E+02 4.84E+01	1.10E−02 1.93E−03	8.34E+09 7.05E+10	7.13E+02 3.76E+01	4.57E+01 2.05E+00	3.00E+08 1.58E+09	2.31E−39 1.63E−39	3.57E+09 1.70E+10
F3	AVG STD	6.54E−37 3.58E−36	5.79E+06 9.08E+05	1.13E+07 1.43E+06	2.98E+06 3.87E+05	5.34E+05 1.34E+05	3.34E+05 7.95E+04	3.37E+07 1.41E+07	1.19E+06 1.88E+05	2.03E+02 2.72E+01	4.90E+06 1.02E+06	1.06E+00 3.70E+00	1.20E+07 1.49E+06
F4	AVG STD	1.29E−47 4.11E−47	9.59E+01 1.20E+00	8.18E+01 9.05E−01	9.35E+01 4.28E+00	4.52E+01 5.72E+00	6.51E+01 3.32E−01	9.82E+01 1.73E+00	5.00E+01 3.03E−02	4.06E−01 4.15E−01	9.88E+01 4.15E−01	4.02E−31 2.67E−31	9.92E+01 2.33E−01
F5	AVG STD	3.10E−01 3.73E−01	1.79E+09 4.11E+08	1.84E+09 1.11E+08	2.07E+08 2.08E+07	3.30E+07 8.76E+06	4.98E+02 5.23E−01	6.94E+09 2.23E+08	2.56E+07 6.14E+06	1.21E+03 7.04E+01	5.01E+09 2.50E+08	4.97E+02 3.07E−01	4.57E+09 1.25E+09
F6	AVG STD	2.94E−03 3.98E−03	6.27E+05 7.43E+04	6.57E+05 3.29E+04	1.68E+05 8.23E+03	8.01E+04 9.32E+03	9.22E+01 2.15E+00	1.53E+06 3.37E+04	6.30E+04 8.91E+03	8.27E+01 2.24E+00	1.16E+06 3.48E+04	7.82E+01 2.50E+00	7.23E+05 3.28E+04
F7	AVG STD	2.51E−04 2.43E−04	9.10E+03 2.20E+03	1.43E+04 1.51E+03	2.62E+03 3.59E+02	2.53E+02 6.28E+01	4.67E−02 1.12E−02	2.23E+04 1.15E+03	3.71E+02 6.74E+01	8.05E+01 1.37E+01	3.84E+04 2.24E+03	1.71E−03 4.80E−04	2.39E+04 2.72E+03
F8	AVG STD	−2.09E+05 2.84E+01	−1.31E+05 2.31E+04	−1.65E+04 9.99E+02	−1.42E+05 1.98E+03	−3.00E+04 3.12E+03	−5.70E+04 1.15E+04	−9.03E+03 2.12E+03	−7.27E+04 1.14E+04	−2.10E+17 5.71E+03	−6.29E+04 1.00E+04	−5.02E+04 1.38E+03	−2.67E+04
F9	AVG STD	0.00E+00 0.00E+00	3.29E+03 1.96E+02	6.63E+03 1.07E+02	7.86E+02 3.42E+01	4.96E+03 7.64E+01	7.84E+01 3.13E+01	6.18E+03 1.20E+02	2.80E+03 1.42E+02	2.54E+03 5.21E+01	6.96E+03 1.48E+02	0.00E+00 0.00E+00	7.14E+03 1.05E+02
F10	AVG STD	8.88E−16 4.01E−31	1.96E+01 2.04E−01	1.97E+01 1.04E−01	1.44E+01 2.22E−01	8.55E+00 8.66E−01	1.93E−03 3.50E−04	2.04E+01 3.25E−02	1.24E+01 4.46E−01	1.07E+00 6.01E−02	2.03E+01 1.48E−01	7.62E−01 2.33E+00	2.06E+01 2.45E−01
F11	AVG STD	0.00E+00 0.00E+00	5.42E+03 7.32E+02	5.94E+03 3.19E+02	1.47E+03 8.10E+01	6.88E+02 8.17E+01	1.55E−02 3.50E−02	1.38E+04 3.19E+02	5.83E+02 7.33E+01	2.66E−02 2.30E−03	1.03E+04 4.43E+02	0.00E+00 0.00E+00	6.75E+03 2.97E+02
F12	AVG STD	1.41E−06 1.48E−06	2.79E+09 1.11E+09	3.51E+09 4.16E+08	1.60E+08 3.16E+07	4.50E+06 4.37E+06	7.42E−01 4.38E−02	1.70E+10 6.29E+08	8.67E+05 6.23E+05	3.87E−01 2.47E−02	1.20E+10 6.82E+08	4.61E−01 2.40E−02	1.60E+10 2.34E+09
F13	AVG STD	3.44E−04 4.75E−04	8.84E+09 2.00E+09	6.82E+09 8.45E+08	5.13E+08 6.59E+07	3.94E+07 1.87E+07	5.06E+01 1.30E+00	3.17E+10 9.68E+08	2.29E+07 9.46E+06	6.00E+01 1.13E+00	2.23E+10 1.13E+00	4.98E+01 9.97E−03	2.42E+10 6.39E+09

Table 6

Results of benchmark functions (F1–F13), with 1000 dimensions.

Benchmark	HHO	GA	PSO	BBO	FPA	GWO	BAT	FA	CS	MFO	TLBO	DE	
F1	AVG STD	1.06E−94 4.97E−94	1.36E+06 1.79E+05	1.36E+06 6.33E+04	6.51E+05 2.37E+04	1.70E+05 2.99E+04	2.42E−01 4.72E−02	3.12E+06 4.61E+04	3.20E+05 2.11E+04	1.65E+01 1.27E+00	2.73E+06 4.70E+04	2.73E−76 7.67E−76	2.16E+06 3.39E+05
F2	AVG STD	2.52E−50 5.02E−50	4.29E+03 8.86E+01	1.79E+10 1.79E+10	1.96E+03 2.18E+01	8.34E+02 8.96E+01	7.11E−01 4.96E−01	1.79E+10 1.79E+10	1.79E+10 1.79E+10	1.02E+02 3.49E+00	1.79E+10 1.79E+10	1.79E+10 1.79E+10	1.79E+10 1.79E+10
F3	AVG STD	1.79E−17 9.81E−17	2.29E+07 3.93E+06	3.72E+07 1.16E+07	9.92E+06 1.48E+06	1.95E+06 4.20E+05	1.49E+06 2.43E+05	1.35E+08 4.76E+07	4.95E+06 7.19E+05	8.67E+02 1.10E+02	1.94E+07 3.69E+06	8.61E−01 1.33E+00	5.03E+07 4.14E+06
F4	AVG STD	1.43E−46 7.74E−46	9.79E+01 7.16E−01	8.92E+01 2.39E+00	9.73E+01 7.62E−01	5.03E+01 5.37E+00	7.94E+01 2.77E+00	9.89E+01 2.22E−01	6.06E+01 2.69E+00	4.44E−01 2.24E−02	9.96E+01 1.49E−01	1.01E−30 5.25E−31	9.95E+01 1.43E−01
F5	AVG STD	5.73E−01 1.40E+00	4.73E+09 9.63E+08	3.72E+09 2.76E+08	1.29E+09 6.36E+07	7.27E+07 1.84E+07	1.06E+03 3.07E+01	1.45E+10 3.20E+08	2.47E+08 3.24E+07	2.68E+03 1.27E+02	1.25E+10 3.15E+08	9.97E+02 2.01E−01	1.49E+10 3.06E+08
F6	AVG STD	3.61E−03 5.38E−03	1.52E+06 1.88E+05	1.38E+06 6.05E+04	6.31E+05 1.82E+04	1.60E+05 1.86E+04	2.03E+02 2.45E+00	3.11E+06 6.29E+04	3.18E+05 2.47E+04	2.07E+02 4.12E+00	2.73E+06 4.56E+04	1.93E+02 2.35E+00	2.04E+06 2.46E+05
F7	AVG STD	1.41E−04 1.63E−04	4.45E+04 8.40E+03	6.26E+04 4.16E+03	3.84E+04 2.91E+03	1.09E+03 3.49E+02	1.47E−01 3.28E−02	1.25E+05 3.93E+03	4.44E+03 4.00E+02	4.10E+02 8.22E+01	1.96E+05 6.19E+03	1.83E−03 5.79E−04	2.27E+05 3.52E+04
F8	AVG STD	−4.19E+05 1.03E+02	−1.94E+05 9.74E+03	−2.30E+04 1.70E+03	−2.29E+05 3.76E+03	−4.25E+04 1.47E+03	−8.64E+04 1.91E+04	−1.48E+04 3.14E+03	−1.08E+05 1.69E+04	−9.34E+14 2.12E+15	−9.00E+04 7.20E+03	−6.44E+04 1.92E+04	−3.72E+04 1.23E+03
F9	AVG STD	0.00E+00 0.00E+00	8.02E+03 3.01E+02	1.35E+04 1.83E+02	2.86E+03 9.03E+01	1.01E+04 1.57E+02	2.06E+02 4.81E+01	1.40E+04 1.85E+02	7.17E+03 1.88E+02	6.05E+03 1.41E+02	1.56E+04 1.94E+02	0.00E+00 0.00E+00	1.50E+04 1.79E+02
F10	AVG STD	8.88E−16 4.01E−31	1.95E+01 2.55E−01	1.98E+01 1.24E−01	1.67E+01 8.63E−02	8.62E+00 9.10E−01	1.88E−02 2.74E−03	2.07E+01 2.23E−02	1.55E+01 2.42E−01	1.18E+00 5.90E−02	2.04E+01 1.26E−01	5.09E−01 1.94E+00	2.07E+01 1.06E−01
F11	AVG STD	0.00E+00 0.00E+00	1.26E+04 1.63E+03	1.23E+04 5.18E+02	5.75E+03 1.78E+02	1.52E+03 2.66E+02	6.58E−02 8.82E−02	2.83E+04 4.21E+02	3.92E+02 1.78E+02	2.47E+04 3.58E−03	1.07E−16 4.51E+02	1.85E+04 2.03E−17	2.22E+03
F12	AVG STD	1.02E−06 1.16E−06	1.14E+10 1.27E+09	7.73E+09 6.72E+08	1.56E+09 1.46E+08	8.11E+06 8.46E+06	1.15E+00 1.82E−01	3.63E+10 1.11E+09	6.76E+07 1.80E+07	6.53E−01 2.45E−02	3.04E+10 9.72E+08	6.94E−01 1.90E−02	3.72E+10 7.67E+08
F13	AVG STD	8.41E−04 1.18E−03	1.91E+10 4.21E+09	1.58E+10 1.56E+09	4.17E+09 2.54E+08	8.96E+07 3.65E+07	1.21E+02 1.11E+01	6.61E+10 1.40E+09	4.42E+08 7.91E+07	1.32E+02 1.48E+00	5.62E+10 1.76E+09	9.98E+01 1.31E−02	6.66E+10 2.26E+09

The results in Table 8 verify that HHO provides superior and very competitive results on F14–F23 fixed dimension MM test cases. The results on F16–F18 are very competitive and all algorithms have attained high-quality results. Based on results in Table 8, the proposed HHO has always achieved to the best results on F14–F23 problems in comparison with other approaches. Based on results for F24–F29 hybrid CM functions in Table 8, the HHO is capable of achieving to high-quality solutions and outperforming other competitors. The p-values in Table 24 also confirm the meaningful advantage of HHO compared to other optimizers for the majority of cases.

4.6. Engineering benchmark sets

In this section, the proposed HHO is applied to six well-known benchmark engineering problems. Tackling engineering design tasks using P-metaheuristics is a well-regarded research direction in the previous works [61,62]. The results of HHO is compared to various conventional and modified optimizers proposed in previous studies. Table 9 tabulates the details of the tackled engineering design tasks.

4.6.1. Three-bar truss design problem

This problem can be regarded as one of the most studied cases in previous works [63]. This problem can be described mathematically as follows:

$$\begin{aligned} \text{Consider } & \vec{X} = [x_1 x_2] = [A_1 A_2], \\ \text{Minimize } & f(\vec{X}) = \left(2\sqrt{2}X_1 + X_2 \right) \times 1, \\ \text{Subject to } & g_1(\vec{X}) = \frac{\sqrt{2}x_1 + x_2}{\sqrt{2}x_1^2 + 2x_1x_2} P - \sigma \leq 0, \\ & g_2(\vec{X}) = \frac{x_2}{\sqrt{2}x_1^2 + 2x_1x_2} P - \sigma \leq 0, \\ & g_3(\vec{X}) = \frac{1}{\sqrt{2}x_2^2 + x_1x_2} P - \sigma \leq 0, \\ \text{Variable range } & 0 \leq x_1, x_2 \leq 1, \\ \text{where } & 1 = 100 \text{ cm}, \quad P = 2 \text{ KN/cm}^2, \quad \sigma = 2 \text{ KN/cm}^2 \end{aligned}$$

Fig. 13 demonstrates the shape of the formulated truss and the related forces on this structure. With regard to Fig. 13 and the

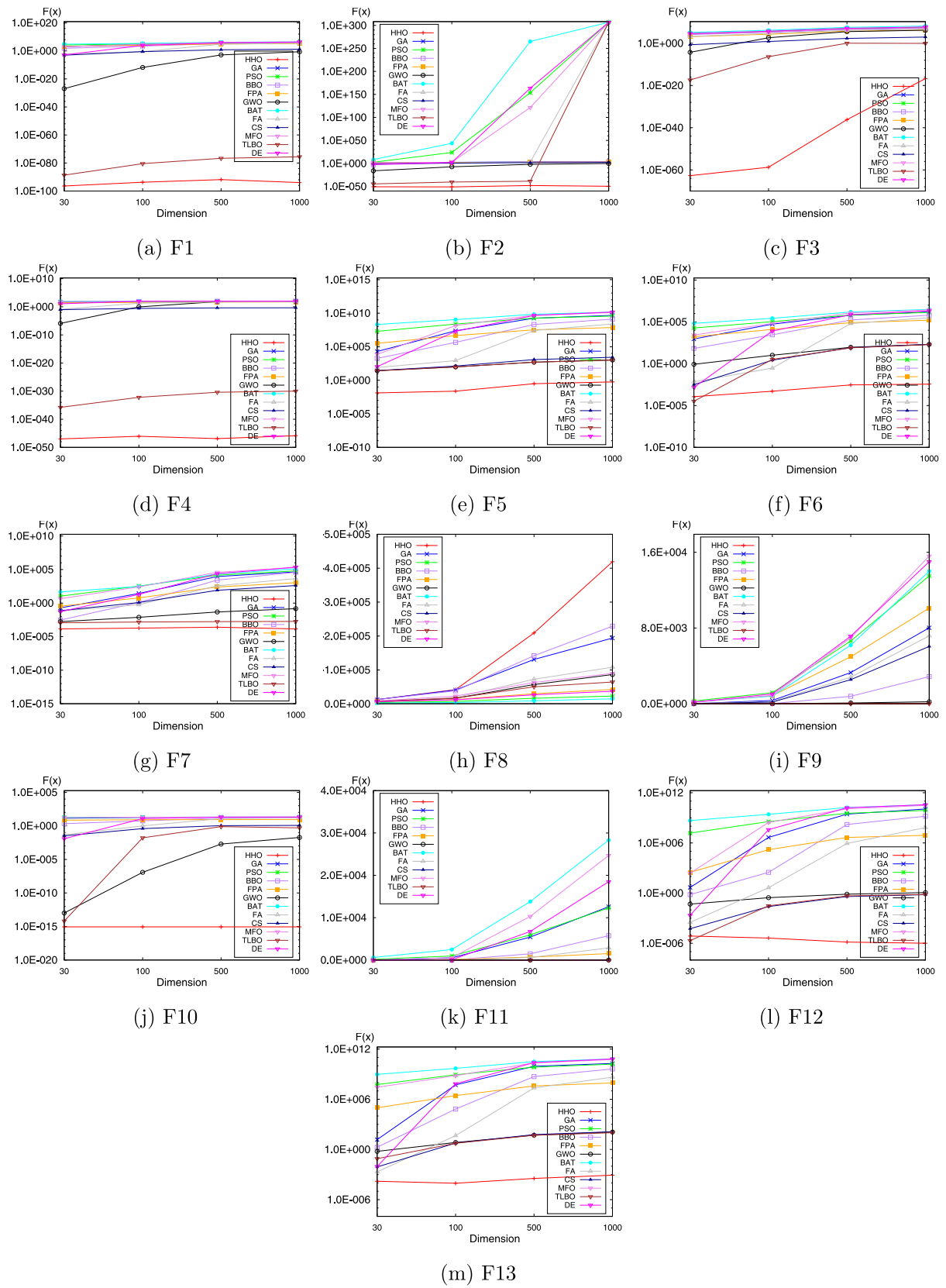


Fig. 12. Scalability results of the HHO versus other methods in dealing with the F1–F13 cases with different dimensions.

formulation, we have two parameters: the area of bars 1 and 3 and area of bar 2. The objective of this task is to minimize the

total weight of the structure. In addition, this design case has several constraints including stress, deflection, and buckling.

Table 7

Comparison of average running time results (seconds) over 30 runs for larger-scale problems with 1000 variables.

ID	Metric	HHO	GA	PSO	BBO	FPA	GWO	BAT	FA	CS	MFO	TLBO	DE
F1	Avg	2.03E+00	8.27E+01	8.29E+01	1.17E+02	2.13E+00	4.47E+00	1.60E+00	5.62E+00	5.47E+00	3.23E+00	2.21E+00	2.38E+00
	Std	4.04E−01	5.13E+00	4.04E+00	6.04E+00	2.62E−01	2.64E−01	2.08E−01	4.42E−01	4.00E−01	2.06E−01	3.62E−01	2.70E−01
F2	Avg	1.70E+00	8.41E+01	8.28E+01	1.16E+02	2.09E+00	4.37E+00	1.61E+00	2.57E+00	5.50E+00	3.25E+00	1.99E+00	2.28E+00
	Std	7.37E−02	4.65E+00	4.08E+00	6.28E+00	8.64E−02	1.29E−01	1.02E−01	3.93E−01	3.48E−01	1.56E−01	1.19E−01	1.16E−01
F3	Avg	1.17E+02	1.32E+02	1.30E+02	1.65E+02	5.10E+01	5.20E+01	5.23E+01	3.70E+01	1.02E+02	5.11E+01	9.76E+01	5.04E+01
	Std	5.28E+00	5.68E+00	5.73E+00	7.56E+00	2.01E+00	1.93E+00	2.25E+00	1.49E+00	3.73E+00	2.00E+00	3.87E+00	1.98E+00
F4	Avg	2.05E+00	8.14E+01	8.24E+01	1.18E+02	1.90E+00	4.27E+00	1.44E+00	5.43E+00	5.14E+00	3.14E+00	1.87E+00	2.21E+00
	Std	7.40E−02	3.73E+00	3.91E+00	5.48E+00	5.83E−02	1.36E−01	1.02E−01	2.76E−01	2.33E−01	9.28E−02	1.05E−01	8.73E−02
F5	Avg	2.95E+00	8.16E+01	8.33E+01	1.17E+02	2.04E+00	4.46E+00	1.65E+00	5.61E+00	5.49E+00	3.31E+00	2.23E+00	2.38E+00
	Std	8.36E−02	4.13E+00	4.36E+00	5.91E+00	7.79E−02	1.39E−01	1.16E−01	3.01E−01	2.74E−01	1.27E−01	1.09E−01	1.30E−01
F6	Avg	2.49E+00	8.08E+01	8.26E+01	1.17E+02	1.88E+00	4.29E+00	1.47E+00	5.51E+00	5.17E+00	3.13E+00	1.89E+00	2.19E+00
	Std	8.25E−02	3.96E+00	3.95E+00	5.69E+00	4.98E−02	1.07E−01	1.03E−01	2.87E−01	2.35E−01	1.00E−01	9.33E−02	1.02E−01
F7	Avg	8.20E+00	8.26E+01	8.52E+01	1.18E+02	4.79E+00	7.08E+00	4.22E+00	6.89E+00	1.08E+01	5.83E+00	7.23E+00	4.95E+00
	Std	1.69E−01	4.56E+00	3.94E+00	6.10E+00	1.02E−01	7.56E−02	8.98E−02	2.02E−01	3.86E−01	1.01E−01	1.31E−01	1.43E−01
F8	Avg	4.86E+00	8.47E+01	8.36E+01	1.18E+02	3.18E+00	5.21E+00	2.45E+00	6.04E+00	7.69E+00	4.05E+00	3.84E+00	3.23E+00
	Std	1.03E+00	3.68E+00	3.80E+00	5.52E+00	4.73E−01	1.78E−01	2.88E−01	2.69E−01	3.86E−01	1.20E−01	4.12E−01	8.69E−02
F9	Avg	3.77E+00	8.09E+01	8.33E+01	1.15E+02	2.84E+00	4.72E+00	2.33E+00	5.89E+00	6.90E+00	3.94E+00	2.70E+00	3.20E+00
	Std	8.87E−01	3.59E+00	3.88E+00	5.94E+00	4.30E−01	1.19E−01	2.88E−01	2.55E−01	3.34E−01	1.26E−01	4.71E−01	5.50E−01
F10	Avg	3.75E+00	8.24E+01	8.36E+01	1.17E+02	2.96E+00	4.80E+00	2.46E+00	5.98E+00	6.56E+00	4.04E+00	2.84E+00	3.41E+00
	Std	8.75E−01	4.02E+00	3.99E+00	5.90E+00	3.74E−01	1.14E−01	4.67E−01	2.91E−01	3.51E−01	1.21E−01	5.39E−01	3.01E−01
F11	Avg	4.17E+00	8.23E+01	8.38E+01	1.18E+02	3.16E+00	4.95E+00	2.61E+00	6.03E+00	6.43E+00	4.22E+00	3.03E+00	3.38E+00
	Std	5.56E−01	4.41E+00	3.97E+00	6.02E+00	5.50E−01	8.65E−02	3.95E−01	2.50E−01	3.01E−01	1.20E−01	3.95E−01	9.95E−02
F12	Avg	1.90E+01	8.64E+01	8.85E+01	1.23E+02	9.09E+00	1.06E+01	8.66E+00	9.17E+00	1.90E+01	9.67E+00	1.53E+01	9.14E+00
	Std	3.31E+00	4.47E+00	4.42E+00	6.20E+00	1.39E+00	4.33E−01	1.47E+00	3.62E−01	3.53E+00	4.04E−01	2.54E+00	1.14E+00
F13	Avg	1.89E+01	8.64E+01	8.90E+01	1.23E+02	9.28E+00	1.05E+01	8.74E+00	9.24E+00	1.83E+01	9.66E+00	1.46E+01	9.34E+00
	Std	1.56E+00	4.40E+00	4.20E+00	6.29E+00	1.50E+00	4.56E−01	1.38E+00	3.94E−01	7.75E−01	3.91E−01	2.24E+00	1.24E+00

Table 8

Results of benchmark functions (F14–F29).

Benchmark	HHO	GA	PSO	BBO	FPA	GWO	BAT	FA	CS	MFO	TLBO	DE	
F14	9.98E−01	9.98E−01	1.39E+00	9.98E−01	9.98E−01	4.17E+00	1.27E+01	3.51E+00	1.27E+01	2.74E+00	9.98E−01	1.23E+00	
	STD	9.23E−01	4.52E−16	4.60E−01	4.52E−16	2.00E−04	3.61E+00	6.96E+00	2.16E+00	1.81E−15	1.82E+00	4.52E−16	9.23E−01
F15	Avg	3.10E−04	3.33E−02	1.61E−03	1.66E−02	6.88E−04	6.24E−03	3.00E−02	1.01E−03	3.13E−04	2.35E−03	1.03E−03	5.63E−04
	Std	1.97E−04	2.70E−02	4.60E−04	8.60E−03	1.55E−04	1.25E−02	3.33E−02	4.01E−04	2.99E−05	4.92E−03	3.66E−03	2.81E−04
F16	Avg	−1.03E+00	−3.78E−01	−1.03E+00	−8.30E−01	−1.03E+00	−1.03E+00	−6.87E−01	−1.03E+00	−1.03E+00	−1.03E+00	−1.03E+00	−1.03E+00
	Std	6.78E−16	3.42E−01	2.95E−03	3.16E−01	6.78E−16	6.78E−16	8.18E−01	6.78E−16	6.78E−16	6.78E−16	6.78E−16	6.78E−16
F17	Avg	3.98E−01	5.24E−01	4.00E−01	5.49E−01	3.98E−01	3.98E−01	3.98E−01	3.98E−01	3.98E−01	3.98E−01	3.98E−01	3.98E−01
	Std	2.54E−06	6.06E−02	1.39E−03	6.05E−02	1.69E−16	1.69E−16	1.58E−03	1.69E−16	1.69E−16	1.69E−16	1.69E−16	1.69E−16
F18	Avg	3.00E+00	3.00E+00	3.10E+00	3.00E+00	3.00E+00	3.00E+00	3.00E+00	1.47E+01	3.00E+00	3.00E+00	3.00E+00	3.00E+00
	Std	0.00E+00	0.00E+00	7.60E−02	0.00E+00	0.00E+00	4.07E−05	2.21E+01	0.00E+00	0.00E+00	0.00E+00	0.00E+00	0.00E+00
F19	Avg	−3.86E+00	−3.42E+00	−3.86E+00	−3.78E+00	−3.86E+00	−3.86E+00	−3.84E+00	−3.86E+00	−3.86E+00	−3.86E+00	−3.86E+00	−3.86E+00
	Std	2.44E−03	3.03E−01	1.24E−03	1.26E−01	3.16E−15	3.14E−03	1.41E−01	3.16E−15	3.16E−15	1.44E−03	3.16E−15	3.16E−15
F20	Avg	−3.322	−1.61351	−3.11088	−2.70774	−3.2951	−3.25866	−3.2546	−3.28105	−3.322	−3.23509	−3.24362	−3.27048
	Std	0.137406	0.46049	0.029126	0.357832	0.019578	0.064305	0.058943	0.063635	1.77636E−15	0.064223	0.15125	0.058919
F21	Avg	−10.451	−6.66177	−4.14764	−8.31508	−5.21514	−8.64121	−4.2661	−7.67362	−5.0552	−6.8859	−8.64525	−9.64796
	Std	0.885673	3.732521	0.919578	2.883867	0.008154	2.563356	2.554009	3.05697	1.77636E−15	3.18186	1.76521	1.51572
F22	Avg	−10.4015	−5.58399	−6.01045	−9.38408	−5.34373	−10.4014	−5.60638	−9.63827	−5.0877	−8.26492	−10.2251	−9.74807
	Std	0.152375	2.605837	1.962628	2.597238	0.356377	1.721889	3.008279	2.345487	1.77636E−15	3.076809	0.007265	1.987703
F23	Avg	−10.5364	−4.69882	−4.72192	−6.2351	−5.29437	−10.0836	−3.97284	−9.75489	−5.1285	−7.65923	−10.0752	−10.5364
	Std	0.927655	3.256702	1.742618	3.78462	0.356377	1.721889	3.008279	2.345487	1.77636E−15	3.576927	1.696222	8.88E−15
F24	Avg	396.8256	626.8389	768.1775	493.0129	518.7886	486.5743	129.1474	471.9752	469.0141	412.4627	612.5569	431.0767
	Std	79.58214	101.2255	76.096491	102.6058	47.84199	142.9028	150.4189	252.1018	60.62538	68.38819	123.2403	64.1864
F25	Avg	910	999.4998	1184.819	935.4693	1023.799	985.4172	1463.423	953.8902	910.1008	947.9322	967.088	917.6204
	Std	0	29.44366	33.02676	9.61349	31.85965	29.95368	68.41612	11.74911	0.036659	27.06282	27.39906	1.052473
F26	Avg	910	998.9091	1178.34	934.2718	1018.002	973.5362	1480.683	953.5493	910.1252	940.1221	983.774	917.346
	Std	0	25.27817	35.20755	34.87908	22.45008	45.55006	14.086	0.047205	21.68256	45.32275	0.897882	
F27	Avg	910	1002.032	1195.088	939.7644	1010.392	969.8538	1477.919	947.7667	910.1233	945.4266	978.7344	917.3067
	Std	0	26.66321	23.97978	23.07814	31.51188	19.51721	60.58827	11.18408	0.049732	26.79031	38.22729	0.861945
F28	Avg	860.8925	1512.467	1711.981	1068.631	1539.357	1337.671	1961.526	1016.389	1340.078	1455.918	1471.879	1553.993
	Std	0.651222	94.64553	35.18377	201.9045	42.93441	191.0662	58.46188	270.6854	134.183	36.06884	268.6238	96.35255
F29	Avg	558.9653	1937.396	2101.145	1897.439	2033.614	1909.091						

Table 10
Comparison of results for three-bar truss design problem.

Algorithm	Optimal values for variables		Optimal weight
	x_1	x_2	
HHO	0.788662816	0.408283133832900	263.8958434
DEDS [64]	0.78867513	0.40824828	263.8958434
MVO [65]	0.78860276	0.408453070000000	263.8958499
GOA [63]	0.788897555578973	0.407619570115153	263.895881496069
MFO [57]	0.788244771	0.409466905784741	263.8959797
PSO-DE [66]	0.7886751	0.4082482	263.8958433
SSA [61]	0.788665414	0.40827578444547	263.8958434
MBA [67]	0.7885650	0.4085597	263.8958522
Tsa [68]	0.788	0.408	263.68
Ray and Sain [69]	0.795	0.395	264.3
CS [34]	0.78867	0.40902	263.9716

Table 11
Comparison of results for tension/compression spring problem.

Algorithms	d	D	N	Optimal cost
HHO	0.051796393	0.359305355	11.138859	0.012665443
SSA [61]	0.051207	0.345215	12.004032	0.0126763
TEO [70]	0.051775	0.3587919	11.16839	0.012665
MFO [57]	0.051994457	0.36410932	10.868422	0.0126669
SFS [71]	0.051689061	0.356717736	11.288966	0.012665233
GWO [56]	0.05169	0.356737	11.28885	0.012666
WOA [18]	0.051207	0.345215	12.004032	0.0126763
Arora [72]	0.053396	0.399180	9.185400	0.012730
GA2 [73]	0.051480	0.351661	11.632201	0.012704
GA3 [74]	0.051989	0.363965	10.890522	0.012681
Belegundu [75]	0.05	0.315900	14.250000	0.012833
CPSO [76]	0.051728	0.357644	11.244543	0.012674
DEDS [64]	0.051689	0.356717	11.288965	0.012665
GSA [25]	0.050276	0.323680	13.525410	0.012702
DELC [77]	0.051689	0.356717	11.288965	0.012665
HEAA [78]	0.051689	0.356729	11.288293	0.012665
WEO [79]	0.051685	0.356630	11.294103	0.012665
BA [80]	0.05169	0.35673	11.2885	0.012665
ESs [81]	0.051643	0.355360	11.397926	0.012698
Rank-iMDDE [82]	0.051689	0.35671718	11.288999	0.012665
CWCA [14]	0.051709	0.35710734	11.270826	0.012672
WCA [62]	0.05168	0.356522	11.30041	0.012665

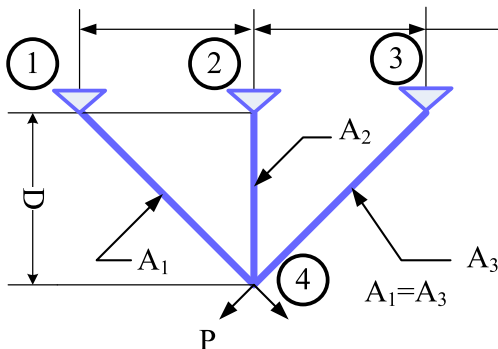


Fig. 13. Three-bar truss design problem.

The HHO is applied to this case based on 30 independent runs with 30 hawks and 500 iterations in each run. Since this benchmark case has some constraints, we need to integrate the HHO with a constraint handling technique. For the sake of simplicity, we used a barrier penalty approach [83] in the HHO. The results of HHO are compared to those reported for DEDS [64], MVO [65], GOA [63], MFO [57], PSO-DE [66], SSA [61], MBA [67], Tsa [68], Ray and Sain [69], and CS [34] in previous literature. Table 10 shows the detailed results of the proposed HHO compared to other techniques. Based on the results in Table 10, it is observed that HHO can reveal very competitive results compared to DEDS, PSO-DE, and SSA algorithms. Additionally, the HHO outperforms

other optimizers significantly. The results obtained show that the HHO is capable of dealing with a constrained space.

4.6.2. Tension/compression spring design

In this case, our intention is to minimize the weight of a spring. Design variables for this case are wire diameter (d), mean coil diameter (D), and the number of active coils (N). For this case, the constraints on shear stress, surge frequency, and minimum deflection should be satisfied during the weight optimization. The objective and constraints of this problem can be formulated as follows:

Consider $\vec{z} = [z_1 z_2 z_3] = [d D N]$,

Minimize $f(\vec{z}) = (z_3 + 2)z_2 z_1^2$,

Subject to

$$g_1(\vec{z}) = 1 - \frac{z_2^3 z_3}{71785 z_1^4} \leq 0,$$

$$g_2(\vec{z}) = \frac{4z_2^2 - z_1 z_2}{12566(z_2 z_1^3 - z_1^4)} + \frac{1}{5108 z_1^2} \leq 0,$$

$$g_3(\vec{z}) = 1 - \frac{140.45 z_1}{z_2^2 z_3} \leq 0$$

$$g_4(\vec{z}) = \frac{z_1 + z_2}{1.5} - 1 \leq 0,$$

There are several optimizers previously applied to this case such as the SSA [61], TEO [70], MFO [57], SFS [71], GWO [56], WOA [18], method presented by Arora [72], GA2 [73], GA3 [74],

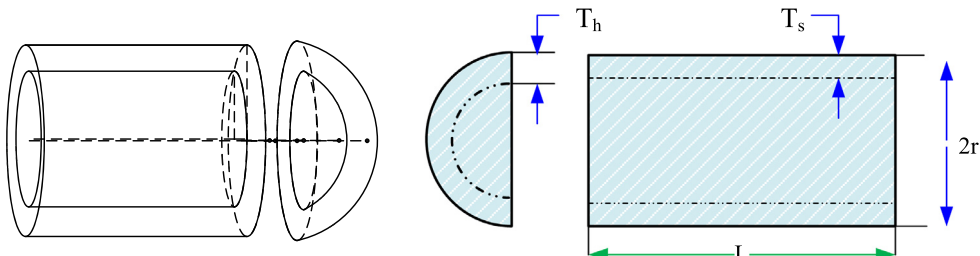


Fig. 14. Pressure vessel problem.

method presented by Belegundu [75], CPSO [76], DEDS [64], GSA [25], DELC [77], HEAA [78], WEO [79], BA [80], ESs [81], Rank-iMDDE [82], CWCA [14], and WCA [62]. The results of HHO are compared to the aforementioned techniques in Table 11.

Table 11 shows that the proposed HHO can achieve to high quality solutions very effectively when tackling this benchmark problem and it exposes the best design. It is evident that results of HHO are very competitive to those of SFS and TEO.

4.6.3. Pressure vessel design problem

In this well-regarded case, we minimize the fabrication cost and it has four parameters and constraints. The variables of this case are ($x_1 - x_4$): $T_s(x_1)$, thickness of the shell, $T_h(x_2)$, thickness of the head, $r(x_3)$, inner radius, $L(x_4)$, length of the section without the head). The overall configuration of this problem is shown in Fig. 14.

The formulation of this test case is as follows:

Consider $\vec{z} = [z_1 z_2 z_3 z_4] = [T_s T_h R L]$,

$$\text{Minimize } f(\vec{z}) = 0.6224z_1z_3z_4 + 1.7781z_2z_2^3 + 3.1661z_1^2z_4 + 19.84z_1^2z_3,$$

Subject to

$$g_1(\vec{z}) = -z_1 + 0.0193z_3 \leq 0,$$

$$g_2(\vec{z}) = -z_3 + 0.00954z_3 \leq 0,$$

$$g_3(\vec{z}) = -\pi z_3^2 z_4 - \frac{4}{3} \pi z_3^3 + 1,296,000 \leq 0,$$

$$g_4(\vec{z}) = z_4 - 240 \leq 0,$$

The design space for this case is limited to: $0 \leq z_1, z_2 \leq 99$, $0 \leq z_3, z_4 \leq 200$. The results of HHO are compared to those of GWO [56], GA [73], HPSO [84], G-QPSO [85], WEO [79], IACO [86], BA [80], MFO [57], CSS [87], ESs [81], CPSO [76], BIANCA [88], MDDE [89], DELC [77], WOA [18], GA3 [74], Lagrangian multiplier (Kannan) [18], and Branch-bound (Sandgren) [18]. Table 12 reports the optimum designs attained by HHO and listed optimizers. Inspecting the results in Table 12, we detected that the HHO is the best optimizer in dealing with problems and can attain superior results compared to other techniques.

4.6.4. Welded beam design problem

Purpose of the well-known engineering case is to discover the best manufacturing cost with regard to a series of design constraints. A schematic view of this problem is illustrated in Fig. 15. The design variables are thickness of weld (h), length (l), height (t), and thickness of the bar (b).

This case can be formulated as follows:

Consider $\vec{z} = [z_1, z_2, z_3, z_4] = [h, l, t, b]$,

$$\text{Minimize } f(\vec{z}) = 1.10471z_1^2z_2 + 0.04811z_3z_4(14.0 + z_2),$$

Subject to

$$g_1(\vec{z}) = \tau(\vec{z}) - \tau_{\max} \leq 0,$$

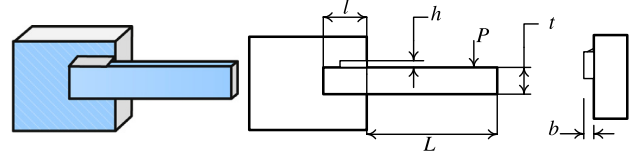


Fig. 15. Welded beam design problem.

$$\begin{aligned} g_2(\vec{z}) &= \sigma(\vec{z}) - \sigma_{\max} \leq 0, \\ g_3(\vec{z}) &= \delta(\vec{z}) - \delta_{\max} \leq 0, \\ g_4(\vec{z}) &= z_1 - z_4 \leq 0, \\ g_5(\vec{z}) &= P - P_c(\vec{z}) \leq 0, \\ g_6(\vec{z}) &= 0.125 - z_1 \leq 0, \\ g_7(\vec{z}) &= 1.10471z_1^2 + 0.04811z_3z_4(14.0 + z_2) - 5.0 \leq 0, \end{aligned}$$

Variable range

$$0.05 \leq z_1 \leq 2.00, \quad 0.25 \leq z_2 \leq 1.30, \quad 2.00 \leq z_3 \leq 15.0,$$

where

$$\begin{aligned} \tau(\vec{z}) &= \sqrt{\tau'^2 + 2\tau'\tau'' \frac{z_2}{2R} + \tau''^2}, \quad \tau' = \frac{P}{\sqrt{2}z_1z_2}, \\ \tau'' &= \frac{MR}{J}, \quad M = P \left(L + \frac{z_2}{2} \right), \\ R &= \sqrt{\frac{z_2^2}{4} + \left(\frac{z_1 + z_3}{2} \right)^2}, \quad J = 2 \left\{ \sqrt{2}z_1z_2 \left[\frac{z_2^2}{12} + \left(\frac{z_1 + z_3}{2} \right)^2 \right] \right\}, \end{aligned}$$

$$\begin{aligned} \sigma(\vec{z}) &= \frac{6PL}{z_4z_3^2}, \\ \delta(\vec{z}) &= \frac{4PL^3}{EZ_3^3z_4}, \quad P_c(\vec{z}) = \frac{4.013E\sqrt{\frac{z_3^2z_4^6}{36}}}{L^2} \left(1 - \frac{z_3}{2L}\sqrt{\frac{E}{4G}} \right), \\ P &= 6000lb, \quad L = 14in, \quad E = 30 \times 10^6 \text{psi}, \quad G = 12 \times 10^6 \text{psi}, \end{aligned}$$

The optimal results of HHO versus those attained by RANDOM [90], DAVID [90], SIMPLEX [90], APPROX [90], GA1 [73], GA2 [83], HS [91], GSA [18], ESs [81], and CDE [92] are represented in Table 13. From Table 13, it can be seen that the proposed HHO can reveal the best design settings with the minimum fitness value compared to other optimizers.

4.6.5. Multi-plate disc clutch brake

In this discrete benchmark task, the intention is to optimize the total weight of a multiple disc clutch brake with regard to five variables: actuating force, inner and outer radius, number of friction surfaces, and thickness of discs [94].

This problem has eight constraints according to the conditions of geometry and operating requirements. The feasible area for this case includes practically 70% of the solution space. However, there are few works that considered this problem in their tests.

Table 12

Comparison of results for pressure vessel design problem.

Algorithms	$T_s(x_1)$	$T_h(x_2)$	$R(x_3)$	$L(x_4)$	Optimal cost
HHO	0.81758383	0.4072927	42.09174576	176.7196352	6000.46259
GWO [56]	0.8125	0.4345	42.089181	176.758731	6051.5639
GA [73]	0.812500	0.437500	42.097398	176.654050	6059.9463
HPSO [84]	0.812500	0.437500	42.0984	176.6366	6059.7143
G-QPSO [85]	0.812500	0.437500	42.0984	176.6372	6059.7208
WEO [79]	0.812500	0.437500	42.098444	176.636622	6059.71
IACO [86]	0.812500	0.437500	42.098353	176.637751	6059.7258
BA [80]	0.812500	0.437500	42.098445	176.636595	6059.7143
MFO [57]	0.8125	0.4375	42.098445	176.636596	6059.7143
CSS [87]	0.812500	0.437500	42.103624	176.572656	6059.0888
ESs [81]	0.812500	0.437500	42.098087	176.640518	6059.7456
CPSO [76]	0.812500	0.437500	42.091266	176.746500	6061.0777
BIANCA [88]	0.812500	0.437500	42.096800	176.6580 0 0	6059.9384
MDDE [89]	0.812500	0.437500	42.098446	176.636047	6059.701660
DELG [77]	0.812500	0.437500	42.0984456	176.6365958	6059.7143
WOA [18]	0.812500	0.437500	42.0982699	176.638998	6059.7410
GA3 [74]	0.812500	0.437500	42.0974	176.6540	6059.9463
Lagrangian multiplier (Kannan) [18]	1.125000	0.625000	58.291000	43.6900000	7198 .0428
Branch-bound (Sandgren) [18]	1.125000	0.625000	47.700000	117.701000	8129.1036

Table 13

Comparison of results for welded beam design problem.

Algorithm	h	l	t	b	Optimal cost
HHO	0.204039	3.531061	9.027463	0.206147	1.73199057
RANDOM [90]	0.4575	4.7313	5.0853	0.66	4.1185
DAVID [90]	0.2434	6.2552	8.2915	0.2444	2.3841
SIMPLEX [90]	0.2792	5.6256	7.7512	0.2796	2.5307
APPROX [90]	0.24 4 4	6.2189	8.2915	0.2444	2.3815
GA1 [73]	0.248900	6.173000	8.178900	0.253300	2.433116
GA2 [83]	0.208800	3.420500	8.997500	0.210000	1.748310
HS [91]	0.2442	6.2231	8.2915	0.2443	2.3807
GSA [18]	0.182129	3.856979	10	0.202376	1.879952
ESs [81]	0.199742	3.61206	9.0375	0.206082	1.7373
CDE [92]	0.203137	3.542998	9.033498	0.206179	1.733462

Table 14

Comparison of results for multi-plate disc clutch brake.

Algorithm	r_i	r_o	t	F	Z	Optimal cost
HHO	69.9999999992493	90	1	1000	2.312781994	0.259768993
TLBO [93]	70	90	1	810	3	0.313656
WCA [62]	70	90	1	910	3	0.313656
PVS [94]	70	90	1	980	3	0.31366

The optimal results of proposed HHO in compared to those revealed by TLBO [93], WCA [62], and PVS [94] algorithms. Table 14 shows the attained results of different optimizers for this test case. From Table 14, we can recognize that the HHO attains the best rank and can outperform the well-known TLBO, WCA, and PVS in terms of quality of solutions.

$$f(x) = \Pi(r_o^2 - r_i^2)t(Z + 1)\rho$$

subject to:

$$g_1(x) = r_o - r_i - \Delta r \geq 0$$

$$g_2(x) = l_{\max} - (Z + 1)(t + \delta) \geq 0$$

$$g_3(x) = P_{\max} - P_{rz} \geq 0$$

$$g_4(x) = P_{\max} v_{sr \max} - P_{rz} v_{sr} \geq 0$$

$$g_5(x) = v_{sr \max} - v_{sr} \geq 0$$

$$g_6 = T_{\max} - T \geq 0$$

$$g_7(x) = M_h - sM_s \geq 0$$

$$g_8(x) = T \geq 0$$

where,

$$M_h = \frac{2}{3}\mu FZ \frac{r_o^3 - r_i^2}{r_o^2 - r_i^3}, \quad P_{rz} = \frac{F}{\Pi(r_o^2 - r_i^2)},$$

$$v_{rz} = \frac{2\Pi n(r_o^3 - r_i^3)}{90(r_o^2 - r_i^2)}, \quad T = \frac{I_z \Pi n}{30(M_h + M_f)}$$

$$\Delta r = 20 \text{ mm}, \quad I_z = 55 \text{ kgmm}^2, \quad P_{\max} = 1 \text{ MPa}, \quad F_{\max} = 1000 \text{ N},$$

$$T_{\max} = 15 \text{ s}, \quad \mu = 0.5, \quad s = 1.5, \quad M_s = 40 \text{ Nm},$$

$$M_f = 3 \text{ Nm}, \quad n = 250 \text{ rpm},$$

$$v_{sr \max} = 10 \text{ m/s}, \quad l_{\max} = 30 \text{ mm}, \quad r_{i \min} = 60,$$

$$r_{i \max} = 80, \quad r_{o \min} = 90,$$

$$r_{o \max} = 110, \quad t_{\min} = 1.5, \quad t_{\max} = 3, \quad F_{\min} = 600,$$

$$F_{\max} = 1000, \quad Z_{\min} = 2, \quad Z_{\max} = 9,$$

4.6.6. Rolling element bearing design problem

This engineering problem has 10 geometric variables, nine constraints considered for assembly and geometric-based restrictions and our purpose for tackling this case is to optimize (maximize) the dynamic load carrying capacity. The formulation of this test case is described as follows:

$$\text{Maximize } C_d = f_c Z^{2/3} D_b^{1.8} \quad \text{if } D \leq 25.4 \text{ mm}$$

$$C_d = 3.647 f_c Z^{2/3} D_b^{1.4} \quad \text{if } D > 25.4 \text{ mm}$$

Subject to

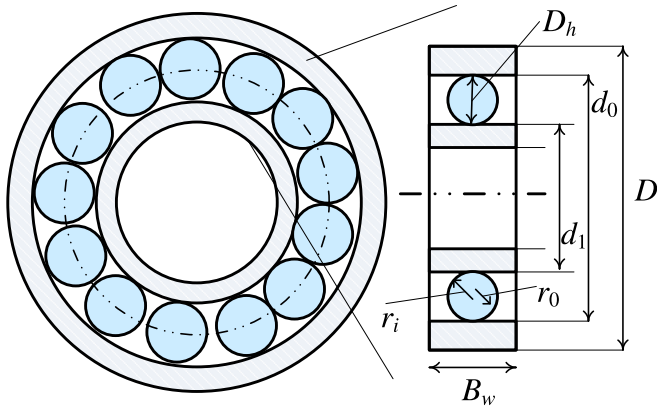


Fig. 16. Rolling element bearing problem.

$$g_1(\vec{z}) = \frac{\phi_0}{2 \sin^{-1}(D_b/D_m)} - Z + 1 \leq 0,$$

$$g_2(\vec{z}) = 2D_b - K_{D\min}(D - d) > 0,$$

$$g_3(\vec{z}) = K_{D\max}(D - d) - 2D_b \geq 0,$$

$$g_4(\vec{z}) = \zeta B_w - D_b \leq 0,$$

$$g_5(\vec{z}) = D_m - 0.5(D + d) \geq 0,$$

$$g_6(\vec{z}) = (0.5 + e)(D + d) - D_m \geq 0,$$

$$g_7(\vec{z}) = 0.5(D - D_m - D_b) - \epsilon D_b \geq 0,$$

$$g_8(\vec{z}) = f_i \geq 0.515,$$

$$g_9(\vec{z}) = f_o \geq 0.515,$$

where

$$f_c = 37.91 \left[1 + \left\{ 1.04 \left(\frac{1-\gamma}{1+\gamma} \right)^{1.72} \left(\frac{f_i(2f_o-1)}{f_o(2f_i-1)} \right)^{0.41} \right\}^{10/3} \right]^{-0.3}$$

$$\times \left[\frac{\gamma^{0.3} (1-\gamma)^{1.39}}{(1+\gamma)^{1/3}} \right] \left[\frac{2f_i}{2f_i-1} \right]^{0.41}$$

$$x = [(D-d)/2 - 3(T/4)]^2$$

$$+ \{D/2 - T/4 - D_b\}^2 - \{d/2 + T/4\}^2]$$

$$y = 2\{(D-d)/2 - 3(T/4)\}\{D/2 - T/4 - D_b\}$$

$$\phi_o = 2\pi - \cos^{-1} \left(\frac{x}{y} \right)$$

$$\gamma = \frac{D_b}{D_m}, \quad f_i = \frac{r_i}{D_b}, \quad f_o = \frac{r_o}{D_b}, \quad T = D - d - 2D_b$$

$$D = 160, \quad d = 90,$$

$$B_w = 30, \quad r_i = r_o = 11.033 \quad 0.5(D+d) \leq D_m \leq 0.6(D+d),$$

$$0.15(D-d) \leq D_b \leq 0.45(D-d), \quad 4 \leq Z \leq 50, \quad 0.515 \leq f_i \\ \text{and } f_o \leq 0.6,$$

$$0.4 \leq K_{D\min} \leq 0.5,$$

$$0.6 \leq K_{D\max} \leq 0.7, \quad 0.3 \leq e \leq 0.4, \quad 0.02 \leq \epsilon \leq 0.1,$$

$$0.6 \leq \zeta \leq 0.85$$

A schematic view of this problem is illustrated in Fig. 16.

This case covers closely 1.5% of the feasible area of the target space. The results of HHO is compared to GA4 [95], TLBO [93], and PVS [94] techniques. Table 15 tabulates the results of HHO versus those of other optimizers. From Table 15, we see that the proposed HHO has detected the best solution with the maximum cost with a substantial progress compared to GA4, TLBO, and PVS algorithms.

5. Discussion on results

As per results in previous sections, we can recognize that the HHO shows significantly superior results for multi-dimensional F1–F13 problems and F14–F29 test cases compared to other well-established optimizers such as GA, PSO, BBO, DE, CS, GWO, MFO, FPA, TLBO, BA, and FA methods. While the efficacy of methods such as PSO, DE, MFO, and GA significantly degrade by increasing the dimensions, the scalability results in Fig. 12 and Table 2 expose that HHO is able to maintain a well equilibrium among the exploratory and exploitative propensities on problem's topographies with many variables. If we observe the results of F1–F7 in Tables 3–6, there is a big, significant gap between the results of several methods such as the GA, PSO, DE, BBO, GWO, FPA, FA, and BA, with high-quality solutions found by HHO. This observation confirms the advanced exploitative merits of the proposed HHO. Based on the solution found for multimodal and hybrid composition landscapes in Table 8, we detect that HHO finds superior and competitive solutions based on a stable balance between the diversification and intensification inclinations and a smooth transition between the searching modes. The results also support the superior exploratory strengths of the HHO. The results for six well-known constrained cases in Tables 10–15 also disclose that HHO obtains the best solutions and it is one of the top optimizers compared to many state-of-the-art techniques. The results highlight that the proposed HHO has several exploratory and exploitative mechanisms and consequently, it has efficiently avoided LO and immature convergence drawbacks when solving different classes of problems and in the case of any LO stagnation, the proposed HHO has shown a higher potential in jumping out of local optimum solutions.

The following features can theoretically assist us in realizing why the proposed HHO can be beneficial in exploring or exploiting the search space of a given optimization problem:

- Escaping energy E parameter has a dynamic randomized time-varying nature, which can further boost the exploration and exploitation patterns of HHO. This factor also requires HHO to perform a smooth transition between exploration and exploitation.
- Different diversification mechanisms with regard to the average location of hawks can boost the exploratory behavior of HHO in initial iterations.
- Different LF-based patterns with short-length jumps enhance the exploitative behaviors of HHO when conducting a local search.
- The progressive selection scheme assists search agents to progressively improve their position and only select a better position, which can improve the quality of solutions and intensification powers of HHO during the course of iterations.
- HHO utilizes a series of searching strategies based on E and r parameters and then, it selects the best movement step. This capability has also a constructive impact on the exploitation potential of HHO.
- The randomized jump J strength can assist candidate solutions in balancing the exploration and exploitation tendencies.
- The use of adaptive and time-varying parameters allows HHO to handle difficulties of a search space including local optimal solutions, multi-modality, and deceptive optima.

Table 15
Comparison of results for rolling element bearing design problem.

Algorithms	GA4 [95]	TLBO [93]	PVS [94]	HHO
D_m	125.717100	125.7191	125.719060	125.000000
D_b	21.423000	21.42559	21.425590	21.000000
Z	11.000000	11.000000	11.000000	11.092073
f_i	0.515000	0.515000	0.515000	0.515000
f_0	0.515000	0.515000	0.515000	0.515000
K_{dmin}	0.415900	0.424266	0.400430	0.400000
K_{dmax}	0.651000	0.633948	0.680160	0.600000
ϵ	0.300043	0.300000	0.300000	0.300000
e	0.022300	0.068858	0.079990	0.050474
ξ	0.751000	0.799498	0.700000	0.600000
Maximum cost	81843.30	81859.74	81859.741210	83011.88329

Table 16
Description of unimodal benchmark functions.

Function	Dimensions	Range	f_{\min}
$f_1(x) = \sum_{i=1}^n x_i^2$	30,100, 500, 1000	[100, 100]	0
$f_2(x) = \sum_{i=1}^n x_i + \prod_{i=1}^n x_i $	30,100, 500, 1000	[10, 10]	0
$f_3(x) = \sum_{i=1}^n \left(\sum_{j=1}^i x_j \right)^2$	30,100, 500, 1000	[100, 100]	0
$f_4(x) = \max_i \{ x_i , 1 \leq i \leq n\}$	30,100, 500, 1000	[100, 100]	0
$f_5(x) = \sum_{i=1}^{n-1} \left[100 (x_{i+1} - x_i^2)^2 + (x_i - 1)^2 \right]$	30,100, 500, 1000	[30, 30]	0
$f_6(x) = \sum_{i=1}^n (x_i + 0.5)^2$	30,100, 500, 1000	[100, 100]	0
$f_7(x) = \sum_{i=1}^n i x_i^4 + \text{random}[0, 1]$	30,100, 500, 1000	[128, 128]	0

Table 17

Description of multimodal benchmark functions.

Function	Dimensions	Range	f_{\min}
$f_8(x) = \sum_{i=1}^n -x_i \sin(\sqrt{ x_i })$	30,100, 500, 1000	[500, 500]	-418.9829 $\times n$
$f_9(x) = \sum_{i=1}^n [x_i^2 - 10 \cos(2\pi x_i) + 10]$	30,100, 500, 1000	[5.12, 5.12]	0
$f_{10}(x) = -20 \exp(-0.2 \sqrt{\frac{1}{n} \sum_{i=1}^n x_i^2}) - \exp\left(\frac{1}{n} \sum_{i=1}^n \cos(2\pi x_i)\right) + 20 + e$	30,100, 500, 1000	[32, 32]	0
$f_{11}(x) = \frac{1}{4000} \sum_{i=1}^n x_i^2 - \prod_{i=1}^n \cos\left(\frac{x_i}{\sqrt{i}}\right) + 1$	30,100, 500, 1000	[600, 600]	0
$f_{12}(x) = \frac{\pi}{n} \left\{ 10 \sin(\pi y_1) + \sum_{i=1}^{n-1} (y_i - 1)^2 [1 + 10 \sin^2(\pi y_{i+1})] + (y_n - 1)^2 \right\} + \sum_{i=1}^n u(x_i, 10, 100, 4)$	30,100, 500, 1000	[50, 50]	0
$y_i = 1 + \frac{x_i+1}{4} u(x_i, a, k, m) = \begin{cases} k(x_i - a)^m & x_i > a \\ 0 - a & < x_i < a \\ k(-x_i - a)^m & x_i < -a \end{cases}$	30,100, 500, 1000	[50, 50]	0
$f_{13}(x) = 0.1 \left\{ \sin^2(3\pi x_1) + \sum_{i=1}^n (x_i - 1)^2 [1 + \sin^2(3\pi x_i + 1)] + (x_n - 1)^2 [1 + \sin^2(2\pi x_n)] \right\} + \sum_{i=1}^n u(x_i, 5, 100, 4)$	30,100, 500, 1000	[50, 50]	0

6. Conclusion and future directions

In this work, a novel population-based optimization algorithm called HHO is proposed to tackle different optimization tasks. The proposed HHO is inspired by the cooperative behaviors and chasing styles of predatory birds, Harris' hawks, in nature. Several equations are designed to simulate the social intelligence of Harris' hawks to solve optimization problems. Twenty nine unconstrained benchmark problems were used to evaluate the performance of HHO. Exploitative, exploratory, and local optima avoidance of HHO was investigated using unimodal, multi-modal and composition problems. The results obtained show that HHO was capable of finding excellent solutions compared to other

well-regarded optimizers. Additionally, the results of six constrained engineering design tasks also revealed that the HHO can show superior results compared to other optimizers.

We designed the HHO as simple as possible with few exploratory and exploitative mechanisms. It is possible to utilize other evolutionary schemes such as mutation and crossover schemes, multi-swarm and multi-leader structure, evolutionary updating structures, and chaos-based phases. Such operators and ideas are beneficial for future works.

In future works, the binary and multi-objective versions of HHO can be developed. In addition, it can be employed to tackle various problems in engineering and other fields. Another interesting direction is to compare different constraint handling strategies in dealing with real-world constrained problems.

Table 18

Description of fixed-dimension multimodal benchmark functions.

Function	Dimensions	Range	f_{\min}
$f_{14}(x) = \left(\frac{1}{500} + \sum_{j=1}^{25} \frac{1}{j + \sum_{i=1}^2 (x_i - a_{ij})^6} \right)^{-1}$	2	[-65, 65]	1
$f_{15}(x) = \sum_{i=1}^{11} \left[a_i - \frac{x_1(b_i^2 + b_i x_2)}{b_i^2 + b_i x_3 + x_4} \right]^2$	4	[-5, 5]	0.00030
$f_{16}(x) = 4x_1^2 - 2.1x_1^4 + \frac{1}{3}x_1^6 + x_1x_2 - 4x_2^2 + 4x_2^4$	2	[-5, 5]	-1.0316
$f_{17}(x) = \left(x_2 - \frac{5.1}{4\pi^2}x_1^2 + \frac{5}{\pi}x_1 - 6 \right)^2 + 10 \left(1 - \frac{1}{8\pi} \right) \cos x_1 + 10$	2	[-5, 5]	0.398
$f_{18}(x) = [1 + (x_1 + x_2 + 1)^2 (19 - 14x_1 + 3x_1^2 - 14x_2 + 6x_1x_2 + 3x_2^2)] \\ \times [30 + (2x_1 - 3x_2)^2 \times (18 - 32x_1 + 12x_1^2 + 48x_2 - 36x_1x_2 + 27x_2^2)]$	2	[-2, 2]	3
$f_{19}(x) = - \sum_{i=1}^4 c_i \exp \left(- \sum_{j=1}^3 a_{ij} (x_j - p_{ij})^2 \right)$	3	[1, 3]	-3.86
$f_{20}(x) = - \sum_{i=1}^4 c_i \exp \left(- \sum_{j=1}^6 a_{ij} (x_j - p_{ij})^2 \right)$	6	[0, 1]	-3.32
$f_{21}(x) = - \sum_{i=1}^5 [(X - a_i)(X - a_i)^T + c_i]^{-1}$	4	[0, 10]	-10.1532
$f_{22}(x) = - \sum_{i=1}^7 [(X - a_i)(X - a_i)^T + c_i]^{-1}$	4	[0, 10]	-10.4028
$f_{23}(x) = - \sum_{i=1}^{10} [(X - a_i)(X - a_i)^T + c_i]^{-1}$	4	[0.10]	-10.5363

Table 19

Details of hybrid composition functions F24–F29 (MM: Multi-modal, R: Rotated, NS: Non-Separable, S: Scalable, D: Dimension).

ID (CEC5-ID)	Description	Properties	D	Range
F24 (C16)	Rotated Hybrid Composition Function	MM, R, NS, S	30	$[-5, 5]^D$
F25 (C18)	Rotated Hybrid Composition Function	MM, R, NS, S	30	$[-5, 5]^D$
F26 (C19)	Rotated Hybrid Composition Function with narrow basin global optimum	MM, NS, S	30	$[-5, 5]^D$
F27 (C20)	Rotated Hybrid Composition Function with Global Optimum on the Bounds	MM, NS, S	30	$[-5, 5]^D$
F28 (C21)	Rotated Hybrid Composition Function	MM, R, NS, S	30	$[-5, 5]^D$
F29 (C25)	Rotated Hybrid Composition Function without bounds	MM, NS, S	30	$[-5, 5]^D$

Table 20

P-values of the Wilcoxon rank-sum test with 5% significance for F1-F13 with 30 dimensions (p-values ≥ 0.05 are shown in bold face, NaN means "Not a Number" returned by the test).

	GA	PSO	BBO	FPA	GWO	BAT	FA	CS	MFO	TLBO	DE
F1	2.85E-11	2.88E-11	2.52E-11	3.02E-11							
F2	2.72E-11	2.52E-11	4.56E-11	3.02E-11							
F3	2.71E-11	2.63E-11	2.79E-11	3.02E-11							
F4	2.62E-11	2.84E-11	2.62E-11	3.02E-11							
F5	2.62E-11	2.52E-11	2.72E-11	3.02E-11							
F6	2.72E-11	2.71E-11	2.62E-11	3.02E-11	3.02E-11	3.02E-11	3.02E-11	3.02E-11	3.02E-11	2.25E-04	3.02E-11
F7	2.52E-11	2.71E-11	9.19E-11	3.02E-11	3.69E-11	3.02E-11	3.02E-11	3.02E-11	3.02E-11	3.02E-11	3.02E-11
F8	7.83E-09	2.71E-11	7.62E-09	3.02E-11							
F9	9.49E-13	1.00E-12	NaN	1.21E-12	4.35E-12	1.21E-12	1.21E-12	1.21E-12	1.21E-12	4.57E-12	1.21E-12
F10	1.01E-12	1.14E-12	1.05E-12	1.21E-12	1.16E-12	1.21E-12	1.21E-12	1.21E-12	1.21E-12	4.46E-13	1.21E-12
F11	9.53E-13	9.57E-13	9.54E-13	1.21E-12	2.79E-03	1.21E-12	1.21E-12	1.21E-12	1.21E-12	NaN	1.21E-12
F12	2.63E-11	2.51E-11	2.63E-11	3.02E-11	3.02E-11	3.02E-11	3.02E-11	1.01E-08	3.02E-11	1.07E-06	3.02E-11
F13	2.51E-11	2.72E-11	2.61E-11	3.02E-11	3.02E-11	3.02E-11	5.49E-11	3.02E-11	3.02E-11	2.00E-06	3.02E-11

Table 21

p-values of the Wilcoxon rank-sum test with 5% significance for F1–F13 with 100 dimensions (p-values ≥ 0.05 are shown in bold face).

Table 22p-values of the Wilcoxon rank-sum test with 5% significance for F1–F13 with 500 dimensions (p-values ≥ 0.05 are shown in bold face).

GA	PSO	BBO	FPA	GWO	BAT	FA	CS	MFO	TLBO	DE
F1	2.94E–11	2.79E–11	2.72E–11	3.02E–11						
F2	2.52E–11	2.63E–11	2.52E–11	3.02E–11						
F3	2.88E–11	2.52E–11	2.72E–11	3.02E–11						
F4	2.25E–11	2.52E–11	2.59E–11	3.02E–11						
F5	2.72E–11	2.72E–11	2.72E–11	3.02E–11						
F6	2.52E–11	2.52E–11	2.52E–11	3.02E–11						
F7	2.52E–11	2.79E–11	2.52E–11	3.02E–11	3.02E–11	3.02E–11	3.02E–11	3.02E–11	4.98E–11	3.02E–11
F8	2.52E–11	2.72E–11	2.63E–11	3.02E–11						
F9	1.06E–12	1.06E–12	1.06E–12	1.21E–12	1.21E–12	1.21E–12	1.21E–12	1.21E–12	Nan	1.21E–12
F10	9.57E–13	9.57E–13	1.06E–12	1.21E–12	1.21E–12	1.21E–12	1.21E–12	1.21E–12	6.14E–14	1.21E–12
F11	9.57E–13	9.57E–13	1.06E–12	1.21E–12	1.21E–12	1.21E–12	1.21E–12	1.21E–12	Nan	1.21E–12
F12	2.52E–11	2.52E–11	2.79E–11	3.02E–11						
F13	2.79E–11	2.52E–11	2.72E–11	3.02E–11						

Table 23p-values of the Wilcoxon rank-sum test with 5% significance for F1–F13 with 1000 dimensions (p-values ≥ 0.05 are shown in bold face).

GA	PSO	BBO	FPA	GWO	BAT	FA	CS	MFO	TLBO	DE
F1	3.01E–11	2.52E–11	2.52E–11	3.02E–11						
F2	2.63E–11	1.21E–12	2.72E–11	3.02E–11	3.02E–11	1.21E–12	3.02E–11	1.21E–12	1.21E–12	1.21E–12
F3	2.86E–11	2.52E–11	2.52E–11	3.02E–11						
F4	1.93E–11	2.52E–11	2.07E–11	3.02E–11						
F5	2.72E–11	2.52E–11	2.52E–11	3.02E–11						
F6	2.63E–11	2.63E–11	2.63E–11	3.02E–11						
F7	2.63E–11	2.52E–11	2.52E–11	3.02E–11						
F8	2.52E–11	2.52E–11	2.52E–11	3.02E–11						
F9	1.01E–12	1.06E–12	9.57E–13	1.21E–12	1.21E–12	1.21E–12	1.21E–12	1.21E–12	Nan	1.21E–12
F10	1.01E–12	1.01E–12	9.57E–13	1.21E–12	1.21E–12	1.21E–12	1.21E–12	1.21E–12	8.72E–14	1.21E–12
F11	1.06E–12	1.01E–12	9.57E–13	1.21E–12	1.21E–12	1.21E–12	1.21E–12	1.21E–12	1.17E–13	1.21E–12
F12	2.52E–11	2.52E–11	2.72E–11	3.02E–11						
F13	2.52E–11	2.63E–11	2.72E–11	3.02E–11						

Table 24p-values of the Wilcoxon rank-sum test with 5% significance for F14–F29 problems(p-values ≥ 0.05 are shown in bold face).

GA	PSO	BBO	FPA	GWO	BAT	FA	CS	MFO	TLBO	DE	
F14	8.15E–02	2.89E–08	8.15E–03	1.08E–01	5.20E–08	7.46E–12	1.53E–09	6.13E–14	9.42E–06	8.15E–02	1.00E+00
F15	2.78E–11	7.37E–11	2.51E–11	9.76E–10	1.37E–01	3.34E–11	3.16E–10	8.69E–10	5.00E–10	5.08E–06	3.92E–02
F16	1.05E–12	9.53E–13	9.49E–13	Nan	Nan	5.54E–03	Nan	Nan	Nan	Nan	Nan
F17	1.87E–12	1.89E–12	2.06E–12	1.61E–01	1.61E–01	5.97E–01	1.61E–01	1.61E–01	1.61E–01	1.61E–01	1.61E–01
F18	Nan	9.53E–13	Nan	Nan	1.09E–02	1.34E–03	Nan	Nan	Nan	Nan	Nan
F19	2.50E–11	5.24E–02	1.91E–09	1.65E–11	1.06E–01	5.02E–10	1.65E–11	1.65E–11	4.54E–10	1.65E–11	1.65E–11
F20	8.74E–03	2.54E–04	8.15E–03	6.15E–03	5.74E–06	5.09E–06	1.73E–07	Nan	1.73E–04	1.73E–04	1.73E–04
F21	1.22E–04	6.25E–05	5.54E–03	1.91E–08	5.54E–03	6.85E–07	1.71E–07	1.91E–08	9.42E–06	1.73E–04	1.79E–04
F22	1.64E–07	5.00E–10	8.15E–08	2.51E–11	8.15E–08	6.63E–07	5.24E–04	1.73E–08	8.15E–08	8.81E–10	1.21E–12
F23	1.54E–05	5.00E–10	8.88E–08	2.51E–11	8.88E–08	1.73E–08	5.14E–04	1.69E–08	8.88E–08	8.81E–10	Nan
F24	2.40E–01	4.69E–08	1.64E–05	1.17E–05	2.84E–04	3.02E–11	3.03E–03	3.08E–08	8.89E–10	8.35E–08	3.20E–09
F25	1.21E–12	1.21E–12	1.21E–12	1.21E–12	1.21E–12	1.21E–12	1.21E–12	1.21E–12	1.21E–12	1.21E–12	1.21E–12
F26	1.21E–12	1.21E–12	1.21E–12	1.21E–12	1.21E–12	1.21E–12	1.21E–12	1.21E–12	1.21E–12	1.21E–12	1.21E–12
F27	1.21E–12	1.21E–12	1.21E–12	1.21E–12	1.21E–12	1.21E–12	1.21E–12	1.21E–12	1.21E–12	1.21E–12	1.21E–12
F28	0.012732	1.17E–09	5.07E–10	0.001114	1.01E–08	3.02E–11	2.37E–10	2.02E–08	8.35E–08	0.446419	2.71E–11
F29	1.85E–08	6.52E–09	3.02E–11	1.29E–06	7.12E–09	3.02E–11	1.17E–09	3.02E–11	3.02E–11	2.6E–08	3.02E–11

Acknowledgments

This research is funded by Zhejiang Provincial Natural Science Foundation of China (LY17F020012), Science and Technology Plan Project of Wenzhou of China (ZG2017019).

We also acknowledge the comments of anonymous reviewers.

Appendix A

See [Tables 16–19](#)

Appendix B

See [Tables 20–24](#)

References

- [1] R. Abbassi, A. Abbassi, A.A. Heidari, S. Mirjalili, An efficient salp swarm-inspired algorithm for parameters identification of photovoltaic cell models, *Energy Convers. Manage.* 179 (2019) 362–372.
- [2] H. Faris, A.M. Al-Zoubi, A.A. Heidari, I. Aljarah, M. Mafarja, M.A. Hassonah, H. Fujita, An intelligent system for spam detection and identification of the most relevant features based on evolutionary random weight networks, *Inf. Fusion* 48 (2019) 67–83.
- [3] J. Nocedal, S.J. Wright, *Numerical Optimization*, 2nd ed., 2006.
- [4] G. Wu, Across neighborhood search for numerical optimization, *Inform. Sci.* 329 (2016) 597–618.
- [5] G. Wu, W. Pedrycz, P.N. Suganthan, R. Mallipeddi, A variable reduction strategy for evolutionary algorithms handling equality constraints, *Appl. Soft Comput.* 37 (2015) 774–786.

- [6] J. Dréo, A.P. étrowski, P. Siarry, E. Taillard, *Metaheuristics for Hard Optimization: Methods and Case Studies*, Springer Science & Business Media, 2006.
- [7] E.-G. Talbi, *Metaheuristics: from Design to Implementation*, vol. 74, John Wiley & Sons, 2009.
- [8] S. Kirkpatrick, C.D. Gelatt, M.P. Vecchi, Optimization by simulated annealing, *Science* 220 (1983) 671–680.
- [9] J.H. Holland, Genetic algorithms, *Sci. Am.* 267 (1992) 66–73.
- [10] J. Luo, H. Chen, Y. Xu, H. Huang, X. Zhao, et al., An improved grasshopper optimization algorithm with application to financial stress prediction, *Appl. Math. Model.* 64 (2018) 654–668.
- [11] M. Wang, H. Chen, B. Yang, X. Zhao, L. Hu, Z. Cai, H. Huang, C. Tong, Toward an optimal kernel extreme learning machine using a chaotic moth-flame optimization strategy with applications in medical diagnoses, *Neurocomputing* 267 (2017) 69–84.
- [12] L. Shen, H. Chen, Z. Yu, W. Kang, B. Zhang, H. Li, B. Yang, D. Liu, Evolving support vector machines using fruit fly optimization for medical data classification, *Knowl.-Based Syst.* 96 (2016) 61–75.
- [13] Q. Zhang, H. Chen, J. Luo, Y. Xu, C. Wu, C. Li, Chaos enhanced bacterial foraging optimization for global optimization, *IEEE Access* (2018).
- [14] A.A. Heidari, R.A. Abbaspour, A.R. Jordehi, An efficient chaotic water cycle algorithm for optimization tasks, *Neural Comput. Appl.* 28 (2017) 57–85.
- [15] M. Mafarja, I. Aljarah, A.A. Heidari, A.I. Hammouri, H. Faris, M. A.-Z. Ala', S. Mirjalili, Evolutionary population dynamics and grasshopper optimization approaches for feature selection problems, *Knowl.-Based Syst.* 145 (2018a) 25–45.
- [16] M. Mafarja, I. Aljarah, A.A. Heidari, H. Faris, P. Fournier-Viger, X. Li, S. Mirjalili, Binary dragonfly optimization for feature selection using time-varying transfer functions, *Knowl.-Based Syst.* 161 (2018b) 185–204.
- [17] I. Aljarah, M. Mafarja, A.A. Heidari, H. Faris, Y. Zhang, S. Mirjalili, Asynchronous accelerating multi-leader salp chains for feature selection, *Appl. Soft Comput.* 71 (2018) 964–979.
- [18] S. Mirjalili, A. Lewis, The whale optimization algorithm, *Adv. Eng. Softw.* 95 (2016) 51–67.
- [19] H. Faris, M.M. Mafarja, A.A. Heidari, I. Aljarah, M. A.-Z. Ala', S. Mirjalili, H. Fujita, An efficient binary salp swarm algorithm with crossover scheme for feature selection problems, *Knowl.-Based Syst.* 154 (2018) 43–67.
- [20] J.R. Koza, *Genetic Programming II: Automatic Discovery of Reusable Subprograms*, MIT Press, Cambridge, MA, 1992.
- [21] R. Storn, K. Price, Differential evolution—a simple and efficient heuristic for global optimization over continuous spaces, *J. Glob. Optim.* 11 (1997) 341–359.
- [22] D. Simon, Biogeography-based optimization, *IEEE Trans. Evol. Comput.* 12 (2008) 702–713.
- [23] O.K. Erol, I. Eksin, A new optimization method: big bang–big crunch, *Adv. Eng. Softw.* 37 (2006) 106–111.
- [24] R.A. Formato, Central force optimization, *Prog. Electromagn. Res.* 77 (2007) 425–491.
- [25] E. Rashedi, H. Nezamabadi-Pour, S. Saryazdi, Gsa: a gravitational search algorithm, *Inf. Sci.* 179 (2009) 2232–2248.
- [26] S. Salcedo-Sanz, Modern meta-heuristics based on nonlinear physics processes: a review of models and design procedures, *Phys. Rep.* 655 (2016) 1–70.
- [27] F. Glover, Tabu search—part i, *ORSA J. Comput.* 1 (1989) 190–206.
- [28] M. Kumar, A.J. Kulkarni, S.C. Satapathy, Socio evolution & learning optimization algorithm: a socio-inspired optimization methodology, *Future Gener. Comput. Syst.* 81 (2018) 252–272.
- [29] R.V. Rao, V.J. Savsani, D. Vakharia, Teaching–learning-based optimization: an optimization method for continuous non-linear large scale problems, *Inform. Sci.* 183 (2012) 1–15.
- [30] A. Baykasoğlu, F.B. Ozsoydan, Evolutionary and population-based methods versus constructive search strategies in dynamic combinatorial optimization, *Inform. Sci.* 420 (2017) 159–183.
- [31] A.A. Heidari, H. Faris, I. Aljarah, S. Mirjalili, An efficient hybrid multilayer perceptron neural network with grasshopper optimization, *Soft Comput.* (2018) 1–18.
- [32] R. Eberhart, J. Kennedy, A new optimizer using particle swarm theory, in: *Micro Machine and Human Science, MHS'95 Proceedings of the Sixth International Symposium on*, IEEE, 1995, pp. 39–43.
- [33] M. Dorigo, V. Maniezzo, A. Colorni, Ant system: optimization by a colony of cooperating agents, *IEEE Trans. Syst. Man Cybern. B* 26 (1996) 29–41.
- [34] A.H. Gandomi, X.-S. Yang, A.H. Alavi, Cuckoo search algorithm: a meta-heuristic approach to solve structural optimization problems, *Eng. Comput.* 29 (2013) 17–35.
- [35] A.A. Heidari, I. Aljarah, H. Faris, H. Chen, J. Luo, S. Mirjalili, An enhanced associative learning-based exploratory whale optimizer for global optimization, *Neural Comput. Appl.* (2019).
- [36] D.H. Wolpert, W.G. Macready, No free lunch theorems for optimization, *IEEE Trans. Evol. Comput.* 1 (1997) 67–82.
- [37] J.C. Bednarz, Cooperative hunting in harris' hawks (*parabuteo unicinctus*), *Science* 239 (1988) 1525.
- [38] S. DeBruyne, D. Kaur, Harris's Hawk multi-objective optimizer for reference point problems, proceedings on the International Conference on Artificial Intelligence (ICAI), in: The Steering Committee of The World Congress in Computer Science, Computer Engineering and Applied Computing (WorldComp), 2016, pp. 287–292.
- [39] L. Lefebvre, P. Whittle, E. Lascaris, A. Finkelstein, Feeding innovations and forebrain size in birds, *Anim. Behav.* 53 (1997) 549–560.
- [40] D. Sol, R.P. Duncan, T.M. Blackburn, P. Cassey, L. Lefebvre, Big brains, enhanced cognition, and response of birds to novel environments, *Proc. Natl. Acad. Sci. USA* 102 (2005) 5460–5465.
- [41] F. Dubois, L.-A. Giraldeau, I.M. Hamilton, J.W. Grant, L. Lefebvre, Distraction sneakers decrease the expected level of aggression within groups: a game-theoretic model, *Am. Nat.* 164 (2004) E32–E45.
- [42] A.A.S. EurekAlertA, Bird iq test takes flight, 2005.
- [43] N.E. Humphries, N. Queiroz, J.R. Dyer, N.G. Pade, M.K. Musyl, K.M. Schaefer, D.W. Fuller, J.M. Brunnschweiler, T.K. Doyle, J.D. Houghton, et al., Environmental context explains Lévy and brownian movement patterns of marine predators, *Nature* 465 (2010) 1066–1069.
- [44] G.M. Viswanathan, V. Afanasyev, S. Buldyrev, E. Murphy, P. Prince, H.E. Stanley, Lévy flight search patterns of wandering albatrosses, *Nature* 381 (1996) 413.
- [45] D.W. Sims, E.J. Southall, N.E. Humphries, G.C. Hays, C.J. Bradshaw, J.W. Pitchford, A. James, M.Z. Ahmed, A.S. Brierley, M.A. Hindell, et al., Scaling laws of marine predator search behaviour, *Nature* 451 (2008) 1098–1102.
- [46] A.O. Gautestad, I. Mysterud, Complex animal distribution and abundance from memory-dependent kinetics, *Ecol. Complex.* 3 (2006) 44–55.
- [47] M.F. Shlesinger, Levy flights: variations on a theme, *Physica D* 38 (1989) 304–309.
- [48] G. Viswanathan, V. Afanasyev, S.V. Buldyrev, S. Havlin, M. Da Luz, E. Raposo, H.E. Stanley, Lévy flights in random searches, *Physica A* 282 (2000) 1–12.
- [49] X.-S. Yang, *Nature-inspired Metaheuristic Algorithms*, Luniver press, 2010.
- [50] X. Yao, Y. Liu, G. Lin, Evolutionary programming made faster, *IEEE Trans. Evol. Comput.* 3 (1999) 82–102.
- [51] J.G. Digalakis, K.G. Margaritis, On benchmarking functions for genetic algorithms, *Int. J. Comput. Math.* 77 (2001) 481–506.
- [52] S. García, D. Molina, M. Lozano, F. Herrera, A study on the use of non-parametric tests for analyzing the evolutionary algorithms' behaviour: a case study on the cec'2005 special session on real parameter optimization, *J. Heuristics* 15 (2009) 617.
- [53] X.-S. Yang, A. Hossein Gandomi, Bat algorithm: a novel approach for global engineering optimization, *Eng. Comput.* 29 (2012) 464–483.
- [54] X.-S. Yang, M. Karamanoglu, X. He, Flower pollination algorithm: a novel approach for multiobjective optimization, *Eng. Optim.* 46 (2014) 1222–1237.
- [55] A.H. Gandomi, X.-S. Yang, A.H. Alavi, Mixed variable structural optimization using firefly algorithm, *Comput. Struct.* 89 (2011) 2325–2336.
- [56] S. Mirjalili, S.M. Mirjalili, A. Lewis, Grey wolf optimizer, *Adv. Eng. Softw.* 69 (2014) 46–61.
- [57] S. Mirjalili, Moth-flame optimization algorithm: a novel nature-inspired heuristic paradigm, *Knowl.-Based Syst.* 89 (2015) 228–249.
- [58] J. Derrac, S. García, D. Molina, F. Herrera, A practical tutorial on the use of nonparametric statistical tests as a methodology for comparing evolutionary and swarm intelligence algorithms, *Swarm Evol. Comput.* 1 (2011) 3–18.
- [59] X.-S. Yang, Firefly algorithm, stochastic test functions and design optimisation, *Int. J. Bio-Inspir. Com.* 2 (2010) 78–84.
- [60] F. Van Den Bergh, A.P. Engelbrecht, A study of particle swarm optimization particle trajectories, *Inf. Sci.* 176 (2006) 937–971.
- [61] S. Mirjalili, A.H. Gandomi, S.Z. Mirjalili, S. Saremi, H. Faris, S.M. Mirjalili, Salp swarm algorithm: a bio-inspired optimizer for engineering design problems, *Adv. Eng. Softw.* (2017).
- [62] H. Eskandar, A. Sadollah, A. Bahreininejad, M. Hamdi, Water cycle algorithm—a novel metaheuristic optimization method for solving constrained engineering optimization problems, *Comput. Struct.* 110 (2012) 151–166.
- [63] S. Saremi, S. Mirjalili, A. Lewis, Grasshopper optimisation algorithm: theory and application, *Adv. Eng. Softw.* 105 (2017) 30–47.
- [64] M. Zhang, W. Luo, X. Wang, Differential evolution with dynamic stochastic selection for constrained optimization, *Inform. Sci.* 178 (2008) 3043–3074.
- [65] S. Mirjalili, S.M. Mirjalili, A. Hatamlou, Multi-versus optimizer: a nature-inspired algorithm for global optimization, *Neural Comput. Appl.* 27 (2016) 495–513.
- [66] H. Liu, Z. Cai, Y. Wang, Hybridizing particle swarm optimization with differential evolution for constrained numerical and engineering optimization, *Appl. Soft Comput.* 10 (2010) 629–640.

- [67] A. Sadollah, A. Bahreininejad, H. Eskandar, M. Hamdi, Mine blast algorithm: a new population based algorithm for solving constrained engineering optimization problems, *Appl. Soft Comput.* 13 (2013) 2592–2612.
- [68] J.-F. Tsai, Global optimization of nonlinear fractional programming problems in engineering design, *Eng. Optim.* 37 (2005) 399–409.
- [69] T. Ray, P. Saini, Engineering design optimization using a swarm with an intelligent information sharing among individuals, *Eng. Optim.* 33 (2001) 735–748.
- [70] A. Kaveh, A. Dadras, A novel meta-heuristic optimization algorithm: thermal exchange optimization, *Adv. Eng. Softw.* 110 (2017) 69–84.
- [71] H. Salimi, Stochastic fractal search: a powerful metaheuristic algorithm, *Knowl.-Based Syst.* 75 (2015) 1–18.
- [72] J.S. Arora, *Introduction To Optimum Design*, 1989, McGraw-Hill Book Company, 1967.
- [73] K. Deb, Optimal design of a welded beam via genetic algorithms, *AIAA J.* 29 (1991) 2013–2015.
- [74] C.A.C. Coello, E.M. Montes, Constraint-handling in genetic algorithms through the use of dominance-based tournament selection, *Adv. Eng. Inform.* 16 (2002) 193–203.
- [75] A.D. Belegundu, J.S. Arora, A study of mathematical programming methods for structural optimization. part i: theory, *Internat. J. Numer. Methods Engrg.* 21 (1985) 1583–1599.
- [76] Q. He, L. Wang, An effective co-evolutionary particle swarm optimization for constrained engineering design problems, *Eng. Appl. Artif. Intell.* 20 (2007) 89–99.
- [77] L. Wang, L.-p. Li, An effective differential evolution with level comparison for constrained engineering design, *Struct. Multidiscip. Optim.* 41 (2010) 947–963.
- [78] Y. Wang, Z. Cai, Y. Zhou, Z. Fan, Constrained optimization based on hybrid evolutionary algorithm and adaptive constraint-handling technique, *Struct. Multidiscip. Optim.* 37 (2009) 395–413.
- [79] A. Kaveh, T. Bakhshpoori, Water evaporation optimization: a novel physically inspired optimization algorithm, *Comput. Struct.* 167 (2016) 69–85.
- [80] A.H. Gandomi, X.-S. Yang, A.H. Alavi, S. Talatahari, Bat algorithm for constrained optimization tasks, *Neural Comput. Appl.* 22 (2013) 1239–1255.
- [81] E. Mezura-Montes, C.A.C. Coello, A simple multimembered evolution strategy to solve constrained optimization problems, *IEEE Trans. Evol. Comput.* 9 (2005) 1–17.
- [82] W. Gong, Z. Cai, D. Liang, Engineering optimization by means of an improved constrained differential evolution, *Comput. Methods Appl. Mech. Engrg.* 268 (2014) 884–904.
- [83] C.A.C. Coello, Use of a self-adaptive penalty approach for engineering optimization problems, *Comput. Ind.* 41 (2000) 113–127.
- [84] Q. He, L. Wang, A hybrid particle swarm optimization with a feasibility-based rule for constrained optimization, *Appl. Math. Comput.* 186 (2007) 1407–1422.
- [85] L. dos Santos Coelho, Gaussian quantum-behaved particle swarm optimization approaches for constrained engineering design problems, *Expert Syst. Appl.* 37 (2010) 1676–1683.
- [86] H. Rosenbrock, An automatic method for finding the greatest or least value of a function, *Comput. J.* 3 (1960) 175–184.
- [87] A. Kaveh, S. Talatahari, A novel heuristic optimization method: charged system search, *Acta Mech.* 213 (2010) 267–289.
- [88] M. Montemurro, A. Vincenti, P. Vanucci, The automatic dynamic penalisation method (adp) for handling constraints with genetic algorithms, *Comput. Methods Appl. Mech. Engrg.* 256 (2013) 70–87.
- [89] E. Mezura-Montes, C. Coello Coello, J. Vel ázquez Reyes, L. Mu ñoz-D ávila, Multiple trial vectors in differential evolution for engineering design, *Eng. Optim.* 39 (2007) 567–589.
- [90] K. Ragsdell, D. Phillips, Optimal design of a class of welded structures using geometric programming, *J. Eng. Ind.* 98 (1976) 1021–1025.
- [91] K.S. Lee, Z.W. Geem, A new structural optimization method based on the harmony search algorithm, *Comput. Struct.* 82 (2004) 781–798.
- [92] F.-z. Huang, L. Wang, Q. He, An effective co-evolutionary differential evolution for constrained optimization, *Appl. Math. Comput.* 186 (2007) 340–356.
- [93] R.V. Rao, V.J. Savsani, D. Vakharia, Teaching-learning-based optimization: a novel method for constrained mechanical design optimization problems, *Comput. Aided Des.* 43 (2011) 303–315.
- [94] P. Savsani, V. Savsani, Passing vehicle search (pvs): a novel metaheuristic algorithm, *Appl. Math. Model.* 40 (2016) 3951–3978.
- [95] S. Gupta, R. Tiwari, S.B. Nair, Multi-objective design optimisation of rolling bearings using genetic algorithms, *Mech. Mach. Theory* 42 (2007) 1418–1443.



Ali Asghar Heidari is now a Ph.D. research intern at Department of Computer Science, School of Computing, National University of Singapore (NUS), Singapore. Currently, he is also an exceptionally talented Ph.D. candidate at the University of Tehran and he is awarded and funded by Iran's National Elites Foundation (INEF). His main research interests are advanced machine learning, evolutionary computation, metaheuristics, prediction, information systems, and spatial modeling. He has published more than 14 papers in international journals such as Information Fusion, Energy Conversion and Management, Applied Soft Computing, and Knowledge-Based Systems.



Seyedali Mirjalili is a lecturer at Griffith University and internationally recognized for his advances in Swarm Intelligence (SI) and optimization, including the first set of SI techniques from a synthetic intelligence standpoint – a radical departure from how natural systems are typically understood – and a systematic design framework to reliably benchmark, evaluate, and propose computationally cheap robust optimization algorithms. Dr Mirjalili has published over 80 journal articles, many in high-impact journals with over 7000 citations in total with an H-index of 29 and G-index of 84. From Google Scholar metrics, he is globally the 3rd most cited researcher in Engineering Optimization and Robust Optimization. He is serving an associate editor of Advances in Engineering Software and the journal of Algorithms.



Hossam Faris is an Associate professor at Business Information Technology department/King Abdullah II School for Information Technology/ The University of Jordan (Jordan). Hossam Faris received his BA, M.Sc. degrees (with excellent rates) in Computer Science from Yarmouk University and Al-Balqa' Applied University in 2004 and 2008 respectively in Jordan. Since then, he has been awarded a full-time competition-based PhD scholarship from the Italian Ministry of Education and Research to pursue his PhD degrees in e-Business at University of Salento, Italy, where he obtained his PhD degree in 2011. In 2016, he worked as a Postdoctoral researcher with [GeNeurateam](#) at the Information and Communication Technologies Research Center (CITIC), University of Granada (Spain). Since 2017, he is leading with Dr. Ibrahim Aljarah the research group of Evolutionary Algorithms and Machine Learning ([Evo-ml](#)). His research interests include: Applied Computational Intelligence, Evolutionary Computation, Knowledge Systems, Data mining, Semantic Web and Ontologies.



Ibrahim Aljarah is an associate professor of BIG Data Mining and Computational Intelligence at the University of Jordan – Department of Information Technology, Jordan. He obtained his bachelor degree in Computer Science from Yarmouk University – Jordan, 2003. Dr. Aljarah also obtained his master degree in computer science and information systems from the Jordan University of Science and Technology – Jordan in 2006. He also obtained his Ph.D. in computer Science from the North Dakota State University (NDSU), USA, in May 2014. Since 2017, he is leading with Dr. Hossam Faris the research group of Evolutionary Algorithms and Machine Learning ([Evo-ml](#)). He organized and participated in many conferences in the field of data mining, machine learning, and Big data such as NTIT, CSIT, IEEE NABIC, CASON, and BIGDATA Congress. Furthermore, he contributed in many projects in USA such as Vehicle Class Detection System (VCDS), Pavement Analysis Via Vehicle Electronic Telemetry (PAVNET), and Farm Cloud Storage System (CSS) projects. He has published more than 50 papers in refereed international conferences and journals. His research focuses on data mining, Machine Learning, Big Data, MapReduce, Hadoop, Swarm intelligence, Evolutionary Computation, Social Network Analysis (SNA), and large scale distributed algorithms.



Majdi Mafarja received his B.Sc in Software Engineering and M.Sc in Computer Information Systems from Philadelphia University and The Arab Academy for Banking and Financial Sciences, Jordan in 2005 and 2007 respectively. Dr. Mafarja did his PhD in Computer Science at National University of Malaysia (UKM). He was a member in Datamining and Optimization Research Group (DMO). Now he is an assistant professor at the Department of Computer Science at Birzeit University. His research interests include Evolutionary Computation, Meta-heuristics and Data mining.



Huiling Chen is currently an associate professor in the department of computer science at Wenzhou University, China. He received his Ph.D. degree in the department of computer science and technology at Jilin University, China. His present research interests center on evolutionary computation, machine learning, and data mining, as well as their applications to medical diagnosis and bankruptcy prediction. He has published more than 100 papers in international journals and conference proceedings, including Pattern Recognition, Expert Systems with Applications, Knowledge-Based Systems, Soft Computing, Neurocomputing, Applied Mathematical Modeling, IEEE ACCESS, PAKDD, and among others.